

**Enhanced biomethane recovery from fat, oil, and grease through co-digestion
with food waste and addition of conductive materials**

By

Bappi Chowdhury

A thesis submitted in partial fulfillment of the requirements for the degree of

Master of Science

In

Environmental Engineering

Department of Civil and Environmental Engineering

University of Alberta

© Bappi Chowdhury, 2020

Abstract

In this study, the effect of conductive additives on co-digestion of fat, oil, and grease (FOG) and food waste (FW) was evaluated. Initially, the biochemical methane potential (BMP) test was conducted for the optimization of the mixing ratio of FW and FOG. The optimal methane production ($800 \text{ L (kg VS)}^{-1}$) was obtained from co-digestion of 70% FW + 30% FOG (w/w), which was 1.2 times and 12 times of that obtained from mono-digestion of FW and FOG, respectively. This optimal mixing ratio was used for subsequent fed-batch studies with the addition of two conductive additives, granular activated carbon (GAC) and magnetite. The addition of GAC significantly shortened the lag phase (from 7 to 3 d), reduced accumulation of various volatile fatty acids (VFAs), and enhanced methane production rate (50-80% increase) compared to the control and magnetite-amended bioreactor. Fourier transformation infrared (FTIR) analysis suggested that the degradation of lipids, protein and carbohydrates was the highest in GAC amended reactor, followed by magnetite and control reactors. GAC addition also enriched more abundant and diverse bacteria and methanogens than control. Magnetite addition also showed similar trends but to a lesser degree. The substantial enrichment of syntrophic LCFA β -oxidizing bacteria (e.g. *Syntrophomonas*) and methanogenic archaea in the GAC-amended bioreactor likely attributed to the superior methanogenesis kinetics in GAC amended bioreactor. Our findings suggest that the addition of GAC could provide a sustainable strategy to enrich kinetically efficient syntrophic microbiome to favor methanogenesis kinetics in the co-digestion of FW and FOG.

Preface

The findings presented in this thesis (Chapter 1, 3, 4, and 5) has been published as Bappi Chowdhury, Long Lin, Bipro Ranjan Dhar, , Mohammad Nazrul Islam, Daryl McCartney, Amit Kumar (2019) “*Enhanced biomethane recovery from fat, oil, and grease through co-digestion with food waste and addition of conductive materials*” in *Chemosphere*, vol. 236 (124362). Bappi Chowdhury was responsible for experimental design, laboratory experiments, data interpretation and analyses. L. Lin assisted in processing of microbial community analysis data. B.R. Dhar directed the study. All authors contributed to the manuscript preparation.

Acknowledgements

I would like to express my deep gratitude to my direct supervisor, Dr. Bipro Dhar, for the supervision and guidance he provided to me during this research work. The constant guidance and interest of my supervisor has helped me a lot throughout my research. His comments, suggestions and inspiring advices have substantially valorized my educational experience and enhanced the research's overall quality.

I would also like to thank Dr. Long Lin for teaching me all the lab techniques and analyses. In addition, thank you Dr. Long Lin for your assistance in processing the microbial ecology data from my first experiment.

Finally, I would also like to thank all my colleagues who have supported me and taught me about lab safety, lab techniques, etc. Thank you, guys.

This research project was financially supported by the Government of Alberta, Natural Sciences and Engineering Research Council of Canada (NSERC), and Future Energy Systems (FES), GHD Canada, Waterloo, Canada.

Table of Contents

Abstract	ii
Preface	iii
Acknowledgments	iv
List of Abbreviations	ix
Chapter 1- Introduction	01
1.1 Background	01
1.2 Specific Objectives	04
1.3 Thesis Organization	04
Chapter 2- Literature Review	06
2.1 Fat, oil and grease	06
2.2 FOG Characterization	09
2.3 Detrimental effects of FOG	12
2.4 Anaerobic co-digestion	14
2.5 Challenges associated with Anaerobic co-digestion of FOG	17
2.6 Co-digestion of FOG	21
2.7 Role of microbial community in anaerobic co-digestion of FOG	25
2.8 Application of conductive materials in anaerobic co-digestion	27
Chapter 3 Materials and Methods	30
3.1 Substrate and Inoculum	30
3.2 Experimental Design	30
3.3 Analytical Methods	32
3.4 Modeling and Statistical Analysis	33
3.5 Microbial Community Analysis	34
Chapter 4 Results and Discussion	36
4.1 Optimization of mixing ratios of FW and FOG	36
4.2 Impact of conductive additives on co-digestion performance	38

4.3 VFA accumulation	41
4.4 Ammonia Nitrogen	42
4.5 FTIR results	43
4.6 Microbial Community	49
Chapter 5 Conclusions and Outlook	57
5.1 Conclusions	57
5.2 Significance of results and outlook	57
5.3. Recommendations	58
References	59
Appendix	76

List of Tables

Table 2.1 Characteristics of FOG collected from various sources.....	11
Table 2.2 FOG co-digestion experiment description.....	22-24
Table 4.1 Results for modified Gompertz model fitting (average of 5 cycles).....	41
Table 4.2 Total microbial abundance and diversity indices from three bioreactors.....	51

List of Figures

Figure 2.1. Major mechanism steps involved in FOG deposition	09
Figure.2.2. Process flow diagram of Anaerobic co-digestion	16
Figure.2.3. Diagram illustrating FOG conversion to Methane.....	17
Figure 3.1. Experimental design of optimization of co-digestion of FOG and FW.....	31
Figure 3.2. Experimental design of addition of conductive materials in co-digestion of FOG and FW.....	32
Figure 3.3 Overhead view of BMP test.....	32
Figure 4.1. Methane production at different mixing ratios of FW and FOG.....	36
Fig 4.2. Effect of different conductive additives on co-digestion of FW and FOG. Note. Control indicate co-digestion (70% FW+30%FOG) without any conductive additives. (a)-(e): Cycle-1 to cycle-5.....	39
Fig 4.3. Accumulation of VFAs concentration from cycle-5.....	42
Fig 4.4. Initial and final ammonia concentration from cycle-5.....	43
Fig 4.5. FTIR spectrum of (a) FW and FOG, and (b) final digestate.....	46
Fig 4.6. Principal component analysis for FTIR spectroscopy results (a) score plot and (b) loading plot of PC1 and PC2 from PCA.....	48
Fig 4.7. Relative abundance of (a) bacterial community at phylum level, (b) bacterial community at genus level and (c) methanogens at genus level. Note: sequences that accounted for less than 1% of their population were grouped into “Others”.....	54-55

List of Abbreviations

BMP- Biochemical methane potential.

FOG- Fat, oil, and grease

FTIR- Fourier-transform infrared spectroscopy.

FW-Food waste

VS- Volatile solids.

TS- Total solids.

TCOD- Total chemical oxygen demand.

SCOD- Soluble chemical oxygen demand.

CSTR- Continuous stirred tank reactor.

UASB- Up-flow sludge blanket reactor.

WWTPs- Wastewater treatment plants.

LCFAs -Long chain fatty acids.

VFAs- Volatile fatty acid

Chapter 1

Introduction

1.1 Background

Biowaste and high-strength wastewater generated from restaurants and food processing industries such as slaughterhouse and dairy farms contain a significant amount of fat, oil and grease (FOG) (Razaviarani and Buchanan, 2015). Currently, direct landfill disposal of FOG has been banned in many municipalities in North American and Europe (He et al., 2011a). FOG has also caused severe blockage and clogging problems in piping systems (J. Hunter Long et al., 2012). However, the potential energy value of FOG generated in urban areas in Europe was estimated at 1000 GWh per year (Wallace et al., 2017). Hence, researchers have been looking for proper ways for the valorization of FOG into value-added bioproducts, such as biogas, biodiesel, etc. (Carrere et al., 2012; Pagés-Díaz et al., 2015). Anaerobic digestion is a widely applied waste-to-biomethane process that has been used for various organic waste streams (Dhar et al., 2012, 2011). The lipid content in FOG has a higher methane potential of $1014 \text{ L (kg VS)}^{-1}$, which is much higher than that of carbohydrates (e.g. $370 \text{ L (kg VS)}^{-1}$ for glucose) and protein $740 \text{ L (kg VS)}^{-1}$ (Angelidaki and Sanders, 2004; Wan et al., 2011). Thus, anaerobic digestion (AD) presents an attractive option for biomethane recovery from FOG. Despite this high potential, utilization of FOG as a feedstock for AD involves several challenges.

In anaerobic digestion of FOG, particulate organics in FOG are hydrolyzed to form glycerol and long-chain fatty acids (LCFAs). Almost 90% of the chemical oxygen demand (COD) of lipid is attained in LCFAs (Yamrot M. Amha et al., 2017). The conversion of LCFAs to methane is mediated by an obligatory syntrophic partnership between syntrophic β -oxidizing bacteria and

methanogens. This syntrophic degradation (LCFAs \rightarrow Acetate + Hydrogen \rightarrow Methane) has often been identified as a rate-limiting step rather than lipid hydrolysis process (Sousa et al., 2009). The accumulation of LCFA may have inhibitory effects on methanogens. Acetoclastic methanogens are considered to be the most sensitive to LCFAs (Ziels et al., 2016), while inhibition of hydrogenotrophic methanogens and syntrophic bacteria have also been suggested in some studies (Palatsi et al., 2010; Rasit et al., 2015).

Consequently, co-digestion of FOG with other complementary feedstocks, and thereby balancing carbohydrate/protein/lipid ratio for efficient methane recovery has received much attention in recent years (Xu et al., 2015a). For instance, several studies have reported enhanced methane production from co-digestion of FOG with sewage sludge in bench scale studies (Davidsson et al., 2008; Girault et al., 2012; Kabouris, * et al., 2008a; Noutsopoulos et al., 2013; Wang et al., 2013). It has been reported that addition of FOG at a volumetric fraction of 20-30% (corresponding to VS fraction of 70%) increased methane production up to 200% in co-digestion with sludge (Kurade et al., 2019). However, food waste (FW) could be considered as another alternative substrate for co-digestion with FOG due to its wide availability (Capson-Tojo et al., 2016). Moreover, food waste usually contains a high concentration of readily degradable organics, such as carbohydrates and proteins (Zhang et al., 2015). However, existing literature provides limited information on the performance of co-digestion of FW and FOG. For instance, further investigation on the optimization of mixing ratio of FW and FOG would be essential for promoting co-digestion of these waste streams to enhance methane production.

Recent studies have suggested that higher abundance of syntrophic β -oxidizing bacteria (e.g., *Syntrophomonas*) would be critically important to enhance anaerobic co-digestion of FOG (Yamrot M. Amha et al., 2017; Ziels et al., 2016). For instance, Ziels et al. (Ziels et al., 2016)

observed a correlation between stable co-digestion performance and FOG to *Syntrophomonas* ratio and suggested that the operation of the digester at longer residence time could lead to higher biomass of slow-growing syntrophic bacteria. Minimizing long residence time requirement is a common techno-economic challenge faced by operators of anaerobic digestion facilities. Thus, the development of other alternative techniques to attain higher abundances of syntrophic LCFA-degradation bacteria could further improve FOG co-digestion performance.

More recently, various conductive materials, such as granular activated carbon (GAC), biochar, magnetite, etc. have been studied for enhancing syntrophic degradation of different volatile fatty acids (VFAs) and alcohols to methane. The addition of conductive additives can improve methanogenesis kinetics due to the establishment of kinetically efficient syntrophic microbiome as well as retention of active biomass (Crest et al., 2018; Dang et al., 2016; Lin et al., 2018a; Zhao et al., 2017b). For instance, studies have demonstrated that enhanced methanogenic degradation of complex organic substrates (e.g., dog food) along with low VFA accumulation waste could be correlated with enrichment of fermentative bacteria in digesters amended with conductive additives (Dang et al., 2017, 2016). It has been suggested that conductive materials could allow direct exchange of electrons between electroactive syntrophic bacteria and archaea that can be coupled with carbon dioxide reduction to methane (Barua and Dhar, 2017; Lovley, 2006). This new syntrophic methanogenesis pathway is called direct interspecies electron transfer (DIET). However, to date, no studies have investigated whether conductive additive could facilitate enrichment of syntrophic microbiome in co-digestion of FOG and FW.

1.2 Specific Objectives

To date no studies have investigated the effect of conductive additives on the anaerobic co-digestion of FOG and FW. Based on the research gaps identified, anaerobic co-digestion of FOG and FW with the addition of conductive additives is a novel concept. Thus, the objectives of my thesis research are as follows:

1. To optimize mixing ratios of FOG and FW for anaerobic co-digestion.
2. To evaluate the impact of conductive materials on anaerobic co-digestion of FOG and food waste.
3. To characterize microbial communities and lipid degradation trend in the co-digestion of FOG and FW.

1.3 Thesis Organization

This dissertation investigates how the presence of conductive additives can influence the performance of anaerobic co-digestion of FOG and FW. The organization of this thesis is as follows. This chapter (Chapter 1) provides an overview of the research gaps and summarizes the specific objectives. Chapter 2 provides a literature review on the current challenges associated with fat, oil and grease (FOG). This review discusses characteristics of FOG, deposition mechanism, operational challenges associated with FOG in anaerobic co-digestion. The role of conductive materials on anaerobic digestion process is also discussed in this chapter. Chapter 3 details the materials and methods that were used to conduct firstly, the BMP tests for optimizing the mixing ratio of FOG and FW under mesophilic conditions (37°C). Secondly, this chapter discussed the materials and methods that were followed to conduct the fed-batch cycle in the presence of conductive materials. Furthermore, this section documents the analytical methods used

in this experiment, including the microbial community analysis, FTIR analysis, and statistical analysis of data used. Chapter 4 presents the results and discussion on the experimental work that has been conducted. Firstly, the performance in terms of methane production of different mixing ratios of FOG and FW are discussed. In the following section, the methane production rate after the addition of two conductive materials (Granular activated carbon and magnetite), are discussed. Impacts of conductive additives on volatile fatty acids accumulation and ammonia concentrations are discussed in the following section. In the following section, microbial communities were analyzed to understand the impacts on diversity and richness of different microbial consortium on GAC and magnetite amended reactors. Finally, FTIR analysis results are discussed to understand the lipid degradation trend in different reactors. Chapter 5 summarizes take-home messages and provides an outlook for future research.

Chapter 2

Literature Review

2.1 Fat, oil and grease

Fat, oil and grease (collectively known as FOG) are lipid abundant waste generated from the kitchen of households, restaurants, dairy and meat processing industries (Alqaralleh et al., 2016). In general, meat processing industries and food manufacturing, such as slaughterhouses, dairy firms are the potential sources of fat, oil and grease (J Hunter Long et al., 2012). Mainly cooking oil, meat fats, dairy products, tallow, gravy, margarine, food scraps, sauces, lard, butter, dressing, deep-fried food, cheeses, etc. are the primary sources of fat, oil and grease. Additionally, they may also be found in mixed greens dressing, sauces, margarine, cheddar, dessert, etc. in fewer amounts. In the past couple of decades, there has been an expansion in the consumption of fast food and processed food. Therefore, consumption of fat and oil is increasing globally (Del Mundo and Sutteerawattananonda, 2017). A recent report (FAO 2016) estimated that fat and oil production would increase globally by 4-5 %. With the increasing population, the number of foodservice establishments is also increasing day by day hence are contributing to more FOG generation (Gross et al., 2017).

FOG originating from food processing industries can be categorized into two forms: grease trap waste and used cooking oil (Salama et al., 2019a; Wallace et al., 2017). Grease waste accumulates on the grease interceptor or grease trap. Grease trap/interceptor is a trapping device of grease and thick oil located either below the sink or below the ground outside housing or food service establishment facilities. Grease trap works as a flow-based gravitational device where suspended solids and grease retained through floatation or sedimentation with the course of time. Grease trap

terminology is more frequently used for a relatively smaller trapping device, located just below the kitchen sink which is capable of accumulating around 55 gallons of waste whereas grease interceptor refers to the large volume in size which can accumulate up to 1000-2000 gallons of waste (Wallace et al., 2017). Fat, oil and grease retained from the trap (known as brown grease) forms multilayers in the trapping device (Da Silva Almeida et al., 2016). The upper layer essentially comprises of remaining fat, floating on the surface of organic-rich water, and the bottom layer consists of a slime mix of food particles and suspended solids (J. Hunter Long et al., 2012).

If left unchecked at source, FOG ends up into the sewer system either by direct dumping or escape from the grease trap. The grease traps are intended to trap most of the FOG coming out from food services establishment effluent before reaching the sewer pipe (Husain et al., 2014). However, the overall efficiency of the grease trap devices depends on how often the abatement tools were pumped for cleaning. In North America, maintenance of the grease trap devices varies among different cities, some of the municipalities pumped out the trapping device when it is 25% filled while some of them clean the device after every 90 days (J Hunter Long et al., 2012). Normally, if there is any delay in cleaning, the abatement tool starts to underperform. Moreover, another reason for FOG escaping from the grease trap device could be, while cleaning with hot water in the kitchen, some of the FOG may melt and emulsify like milk within the effluent stream and thus escape through the grease trap device (Husain et al., 2014). FOG shows adhesion towards sewer pipelines under low temperature and due to hydraulic pressure of sewage (Gross et al., 2017). It has the ability to solidify under aforementioned condition and can work as a sticky agent. Over the time, FOG accumulates at sewer interior and starts to hold other solids such as wet wipes, sanitary items, etc. to form large mass of solid waste known as 'fatberg' (Wallace et al., 2017).

The FOG deposition, which leads to fatberg formation, was investigated in previous studies (Gross et al., 2017; He et al., 2017, 2013). Studies have reported calcium ion along with palmitic acid, and oleic acids (free fatty acids) would be the main contributing factors in FOG deposition (Del Mundo and Sutheerawattananonda, 2017; Kevin M. Keener et al., 2008). Keener et al. (2008) identified that calcium concentrations in FOG deposit were well above the hardness of the water. The free fatty acids, such as palmitic acid and oleic acid, are hydrolyzed products of oil generated due to natural biodegradation, whereas the presence of calcium ion results from water hardness, corrosion in sewer pipes due to microbial activity (Wallace et al., 2017).

It has been already reported in a few studies that FOG deposition is mainly a saponification reaction (He et al., 2013, 2011b; Kevin M. Keener et al., 2008). For the saponification process to happen, the alkaline environment is necessary. Therefore, pH is an important parameter in terms of FOG deposition mechanism. During the FOG saponification process, detergents and sanitizers provide an alkaline environment. During the cleaning process in the kitchen or restaurants, FOG is removed from the dishware and mixes with excess cleaning products and sanitizers to form metallic soaps (He et al., 2011b; Keener et al., 2008; Wallace et al., 2017). The result from these studies also reported a high concentration of saturated fatty acids and calcium ion's presence in the FOG deposit. In another study conducted by (He et al., 2013) mentioned about four key components of FOG deposit. The four key components are water, calcium ion, free fatty acids, and FOG. This study also demonstrated key mechanisms involved in FOG deposition. According to previous studies (He et al., 2013; Williams et al., 2012), the formation of FOG deposit involves three keys steps (see Figure 1). In first step, Calcium ion present in the wastewater compresses the double layer, then in the next step saponification reaction happens. Detail reaction is provided in the appendix section. Finally,

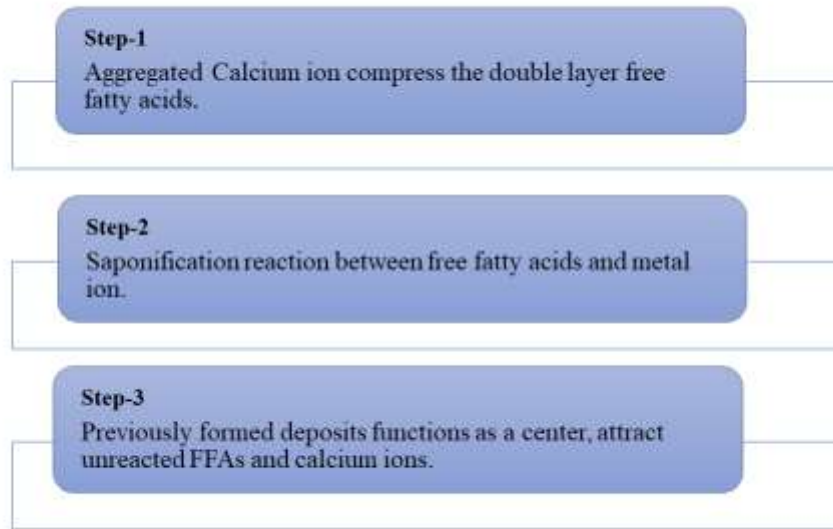


Figure 2.1. Major mechanism steps involved in FOG deposition.

He et al. (2013) also demonstrated the role of concrete corrosion in FOG deposition. Moreover, to get more insight into what is happening in FOG deposition Iasmin et al. (2016) examined the specific chemical breakdown of different FOG streams. They scrutinized the role of pH, fat type, source of metals (calcium, magnesium, sodium) on FOG deposition kinetics. This study helped in better understanding and predicting FOG formation in the sewer system, which could assist in developing sewer system spatial FOG formation modeling.

2.2 FOG Characterization

FOG may occur as a solid or liquid depending mainly on the saturation of the carbon chain. Fat and oil are derivatives of lipids, consisting mainly of fatty acids, triacylglycerols, and natural soluble hydrocarbons. Therefore, FOG mainly comprises of long-chain fatty acids (LCFAs) that are bonded with glycerol, esters, phospholipids, sterols, ester waxes (Husain et al., 2014). The

viscosity of FOG correlates with the concentration of unsaturated fatty acids in the composition of triglyceride ester – the higher the concentration, the lower the viscosity of FOG (Husain et al., 2014). As previously mentioned, FOG generated from restaurants, dairy firms and food processing industries can be categorized into grease trap waste (GTW) and used cooking oil. GTW has high fat content; mainly the presence of saturated fat palmitic acid, unsaturated fat oleic acid, and polyunsaturated fat linoleic acid has been reported in several studies (J Hunter Long et al., 2012). This study also reported that oleic acid is the most common form of long-chain fatty acid, which has been traced in GTW. This finding also agreed with another study conducted by Viswanathan et al. (n.d.) who reported oleic acid as the most abundant form of acid found in wastewater treatment plants. Overall, GTW has FFA (free fatty acid) content of more than 15% (Wallace et al., 2017). Study suggested raw GTW comprised of 4.23% of FOG, 86.35% water and solid concentration of 9.42% (Tu and McDonnell, 2016). This percentage may vary depending on the pump out of the grease interceptor and the grease properties (J Hunter Long et al., 2012). GTW has high biochemical oxygen demand, the majority portion of lipid contains (4.5-6.5 KW h/Kg) energy (J Hunter Long et al., 2012). Dewatered form of GTW is known as FOG . Due to high energy potential, GTW may be utilized to recover energy by means of biodiesel production, anaerobic co-digestion. Due to the presence of a high concentration of saturated and unsaturated acids FOG has high volatile solids (VS) content, which obviously leads to high total chemical oxygen demand (TCOD) as well (Salama et al., 2019a). The physical and chemical characteristics of FOG can vary depending on the sources of generation. Table 1 summarizes characteristics of FOG used in previous anaerobic digestion related studies.

Table:2.1. Characteristics of FOG collected from various sources.

Parameters	FOG (Kabouris, et al., 2008a)	FOG (Wan et al., 2011)	FOG (Tandukar and Pavlostathis, 2015)	FOG (Martín-González et al., 2011)	FOG (Wang et al., 2013)	FOG (Xu et al., 2015b)	FOG (Li et al., 2011a)	FOG (Chowdhury et al., 2019)	FOG (C. Li et al., 2015)	FOG (Kurade et al., 2019)
TS	424 (g/Kg)	3.2 (%, dry base)	155 g/L	116.6 (g/Kg)	968 (g/Kg)	724.5 (g/Kg)	947 (mg/g substrate)	192 (mg/Kg)	966 (g/L)	954 ± 11.1 (g/L)
VS	409 (g/Kg)	3.1 (%, dry base)	126 g/L	103.9 (g/Kg)	955 (g/Kg)	718 (g/L)	942 (mg/g substrate)	175 (mg/Kg)	941 (g/L)	923 ± 1.15 (g/L)
VS/TS (%)	96.5	93.9	81.3	89.1	99.9	99	99.6	97	94 %	97%
pH	4.03	4.2	5.2	N/A	N/A	N/A	4.0	5.15	4.1	4.65
TCOD	1211 g/Kg	N/A	253.7 g/L	N/A	>1500 g/L	N/A	N/A	289 g/L	-	-
VFAs	3472 (g/COD L)	0.8574 (g/L)	3.60 (g/COD L)	NM	NM	63712 g/L	N/A	N/A	890 (mg/L)	-

TS: Total solids; VS: Volatile solids; VFA: Volatile fatty acid; TCOD: Total Chemical Oxygen Demand

2.3 Detrimental effects of FOG

FOG's negative impacts range from local issues such as blocking domestic kitchen pipe to the sewer system's complete disruption. According to a report from the National Renewable Energy Laboratory (NREL) in the USA, the FOG generation rate per year is 1.9 gallons/ person (J Hunter Long et al., 2012). This report was based on a survey conducting in thirty USA metropolitan area. Later on, (US EPA, 2004) published another report on fat, oil and grease deposit, where it is estimated that fat, oil and grease deposits are the prior reason of 40-50% of sewer blockage which later led to sewer overflow in different cities of the USA (Gross et al., 2017). This report also stated that 138000 sanitary overflows happened annually due to the pipes clogged from aggregations of solidified and insoluble FOG deposition (Gross et al., 2017). As mentioned in the previous section, solidified FOG is termed as 'fatberg'. A combination of FOG and fatberg can cause full blockage and spill of sanitary sewer. To address such problem, temporary road closure requires sewage pipeline repair. Moreover, the overflow of sewers can possibly discharge high concentrations of pathogens, supplements, and solids to water bodies that can impose hazards on human health and the earth (Bridges, 2003). It has already been reported in the UK approximately 24750 incidents of line blockages happened per year, and it is also estimated that 50-70% line blockages occurred due to FOG deposition. In another study conducted by (Williams et al., 2012) expressed that FOG consumption in developed countries is significantly higher, approximately 50kg/annum. In contrast, for less developed countries, the number is less than 20 Kg/annum. In the year of 2015, European Biomass Industry Association initiated a project named 'Recoil Project' where they investigated the cooking oil usage in domestic purposes and found out that 2.5L of used cooking oil generated per person per year (Wallace et al., 2017). According to a report from Metro Vancouver, it was estimated that 1019 tonnes of FOG per year ended up getting into

the sewer of this region. It was also stated in that report that four categories of FOG ‘Dairy products and eggs;’ ‘Oil and fat;’ ‘Composite meals’ and ‘Condiments, sauces, herbs, spices;’ contributed to the maximum loadings of FOG in wastewater system in Vancouver. The following section will discuss in detail about the detrimental effects of FOG in various sectors.

Direct release of FOG into the collection system may accumulate in the piping system over the years, could possibly create sticky hard grease balls through physical interaction or chemical reaction (He et al., 2011a). These accumulated portions of FOG could clog pipes, hinder the transport of wastewater stream, ultimately results in sewer backup and spills. FOG can significantly reduce sewer diameter which can lead to sewer overflows (Salama et al., 2019a). (Salama et al., 2019a). A study fabricated in the USA revealed that FOG mainly accumulates 50 m to 200 m downstream from where the FOG originates (Kevin M Keener et al., 2008).

Moreover, most of the sewer system in many countries are relatively older and with time being FOG deposition make it even worse. Upgrading the sewer network needs a significant amount of budget allocation, which is not economically feasible for many countries. For example, the sewer system of the UK is considered to be one of the oldest in the world where the majority portion of sewer systems built around early in the nineteenth and twenty centuries (Wallace et al., 2017). To replace this old sewer system in the UK it will cost about £104 billion, while the UK's estimated cost of maintaining the sewer system varies between £ 15 million to £ 50 million (Pastore et al., 2015). It was reported that the estimated annual expense of wastewater rehabilitation in the USA was nearly \$25 billion (He et al., 2017). In another study, it was mentioned that FOG was the primary cause of 21% of all sewer blockages in Australia (Marlow et al., 2011). In another study focusing on Hong Kong restaurants, wastewater management reported that in the year 2000, 60% of the sewer overflow occurred due to excessive grease build-ups while FOG accounted for up to

70% of SSOs in Malaysia (Husain et al., 2014). Consequently, FOG became a global challenge to maintain wastewater transportation in the sanitary sewer system.

FOG may go through the sewer system and enter WWTPs, where it can overload the system. Though FOG is primarily separated in primary skimming tanks, the portion that is not removed in the skimming tank can cause blockage to the plant pipelines, which eventually results in process interruption in settlement and clarification facilities (Wallace et al., 2017). There are specific techniques available for removal of FOG from the wastewater stream, such as air flotation removed, centrifugation, filtration, microbial extraction, and ultrafiltration (Husain et al., 2014). Some of the techniques of the FOG removal are expensive as well. According to the European Biomass Industry Association in 2015, 25% of the sewage treatment cost was because of the presence of FOG component in the stream (Wallace et al., 2017). Another major problem associated with FOG accumulation in WWTPs is the slow degradation of FOG can affect the activity of microorganisms by preventing sufficient oxygen exchange for degradation of organic waste. If FOG is not removed from wastewater, it will end up in discharge with treated water which will affect the whole waterbodies.

2.4 Anaerobic co-digestion

Anaerobic digestion is a complex biological process that transforms organic substrates (carbohydrates, proteins, and lipids) into biomethane through various biochemical reactions driven by the microorganism (J. Mata-Alvarez et al., 2014). The anaerobic co-digestion involves multiple substrates so that biomethane production can be upgraded due to their complementary characteristics (Salama et al., 2019a). The anaerobic co-digestion is not just assimilation of wastes (substrates); rather the main focus of co-digestion is to achieve optimum blend ratios in order to

promote positive synergies, the balance of nutrients, and dilution of various inhibitory compounds (J Mata-Alvarez et al., 2014).

Biomethane production through co-digestion of FOG is accomplished by the synchronous activities of three groups of microorganisms known as hydrolytic, fermentative (acidogenic and acetogenic) and methanogenic archaea (Madsen et al., 2011). The initial step of anaerobic digestion is hydrolysis where hydrolytic group of bacteria which belong to proteobacteria, Firmicutes, Bacteroidetes phyla; hydrolyze insoluble organic compounds such as carbohydrates, proteins, and fats into soluble monosaccharides, amino acids, LCFAs, and glycerol in presence of water (Salama et al., 2019a). Hydrolysis could be a relatively slow process depending on the characteristics of substrates. During anaerobic co-digestion, the hydrolysis rate depends on different parameters such as pH, the particle size of substrates, enzyme transport to substrates (Salama et al., 2019a). Hydrolysis is immediately followed by acidogenesis where acidogenic bacteria play a vital role in converting hydrolyzed organics to a relatively higher number of carbon-containing organic acids, such as propionate, butyrate, pyruvate, succinate, and lactate (Ostrem., 2004). This step also additionally produces alcohols (methanol and ethanol), CO₂, and H₂. In the next step, higher organic acid subsequently converted to acetic acid and hydrogen by acetogenic bacteria. This step is known as the acetogenic step (Salama et al., 2019a). A clear distinction between acetogenic and acidogenic reaction is not always possible as both of the processes happen simultaneously in the presence of a diverse group of facultative and obligate anaerobes. Species responsible for acidogenesis are mainly *Enterobacteriaceae*, *Clostridia*, *Bacillus*, and *Bacteroides* etc. In the final step methanogens produce methane by utilizing (acetate, CO₂, H₂). It was reported that approximately 70% methane production comes from acetoclastic pathway where

methanogens utilize acetate to form methane (Salama et al., 2019a). **Figure.2.2.** summarizes various steps involved in anaerobic digestion.

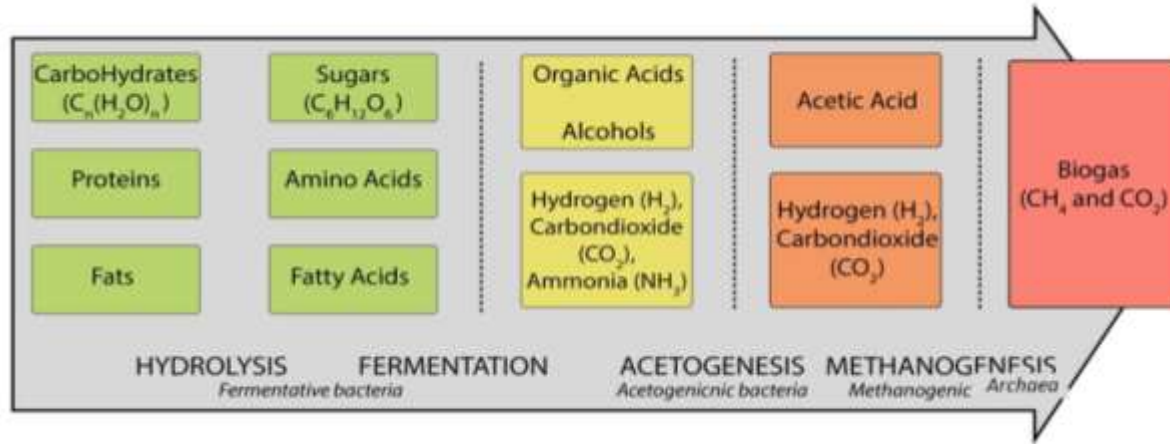


Figure 2.2. Process flow diagram of Anaerobic co-digestion

When FOG (fat, oil and grease) introduced in anaerobic digestion or co-digestion system, they are hydrolyzed to form glycerol and long-chain fatty acid (LCFA). Hydrolysis is one of the rates limiting steps of AD or ACo-D process. Almost 90% of Chemical oxygen demand of lipid is distributed in LCFA (Yamrot M. Amha et al., 2017). Therefore, the success of the AD process depends on the degradation of LCFA. LCFA anaerobically degraded through beta-oxidation pathway to form acetate and hydrogen. Beta oxidation mechanism starts with the activation of coenzyme-A, following on the release of acetyl Co-A, which enters the citric acid cycle to degrade LCFA (J. Hunter Long et al., 2012). Though saturated long-chain fatty acid follows the conventional beta-oxidation mechanism, there is still an ongoing debate about the unsaturated LCFA degradation mechanism. One proposed mechanism is that unsaturated LCFA first converts to saturated LCFA by hydrogenation and then proceed to further degradation (Sousa et al., 2009). Another study suggested that beta-oxidation of unsaturated acid occurs before fatty acid saturation (Roy et al., 1986). It was evident from multiple studies that the degradation of oleic acid produces

intermediate palmitic acid. However, the degradation of oleic (C18:1) and linoleic (C18:2) acid degrades to palmitic acid (C16:0) with no intermediate stearic acid (C18:0) was detected indicating the fact that unsaturated fatty acid may not require complete fatty acid saturation prior to beta-oxidation (J. Hunter Long et al., 2012). The following reaction expresses the beta-oxidation pathway for LCFA degradation.

LCFA degradation overall reaction:

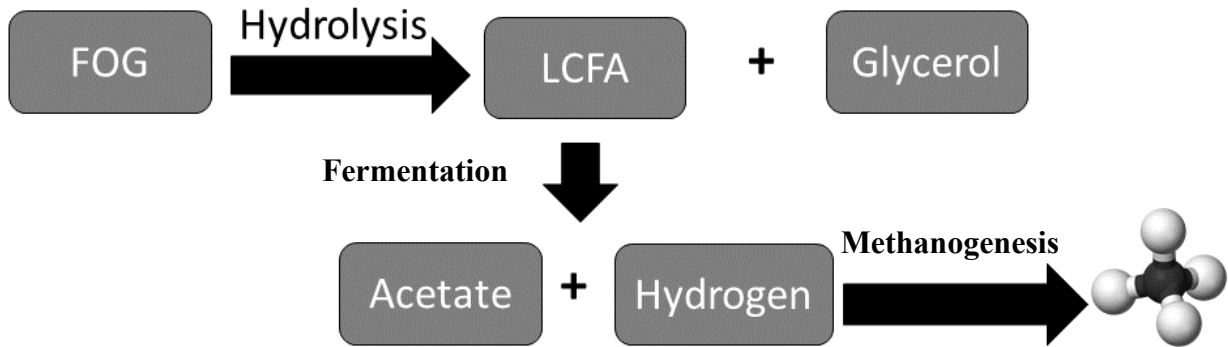


Figure 2.3. Diagram illustrating FOG conversion to Methane.

2.5 Challenges associated with Anaerobic co-digestion of FOG

One major concern of co-digestion with FOG is that it can have an inhibitory effect on methanogenic microorganism as the hydrolysis of FOG forms long-chain fatty acid (M Madalena Alves et al., 2009). Acetoclastic methanogens are considered to be the most sensitive towards LCFA (Ziels et al., 2016). Inhibition of hydrogenotrophic methanogens and syntrophic bacteria has also been reported in many studies (Palatsi et al., 2010; Rasit et al., 2015). This inhibition is

more prominent if a high organic loading rate is applied in the system (J. Hunter Long et al., 2012; Ziels et al., 2016). Several studies with anaerobic co-digestion of FOG reported some reasons for inhibition due to LCFAs. LCFAs works as a barrier between cell and substrate. LCFAs may create a coat on the surface of the bacteria, which may cause nutrient transport limitation to the microbes (Yamrot M. Amha et al., 2017). LCFA also has a toxicity effect if it presents in high concentration (Ziels et al., 2016). Digester foaming, sludge flotation and washout are some other operational concerns related to anaerobic co-digestion of FOG. All these inhibition mechanisms were identified in various types of reactors like EGSB, UASB with batch, semi-continuous, or continuous system. The substrates and products transport limitations can vary depending on the digester design. A stronger mixing condition in the CSTR is reported to degrade higher lipids (63–68%) compared to that in the UASB reactor (48–67%) (Salama et al., 2019b). This section will discuss in detail about the challenges of anaerobic co-digestion with FOG.

Many researchers investigated that LCFAs have inhibitory effects on methanogenic archaea activity. Though there is evidence of toxicity effect of LCFAs, it is still not that much clear how LCFAs impose an adverse effect on methanogenic archaea. However, initial research suggested that LCFAs could work as a surfactant agent, which could potentially desecrate the outer cell surface (J. Hunter Long et al., 2012; Palatsi et al., 2010). LCFAs function as a surface tension reducing agent, which may cause irreversible change to the cell membrane in a way that proton transfer can occur both ways. Injury to the cell wall can also lead to the inability of the microorganism to manage the energy flow, which means that ATP synthesis will be interrupted (Yamrot M. Amha et al., 2017). At first (Coles and Lichstein., 1963) proposed that oleic acid, most common form of LCFA found in wastewater treatment, could affect the permeability of the cell membrane, which resulted in a pH imbalance in the digester. Process instability observed at higher

FOG loading in several studies, which attributed to less methane production than the theoretical one (Alqaralleh et al., 2016; Rasit et al., 2015; Rinzema et al., 1994). (Hanaki et al., 1981) stated that in case of shock loading of LCFAs, anaerobic digestion could be completely stopped. This study also identified that higher loading of LCFAs contributed to the increasing lag phase in the anaerobic process. Few studies suggested a correlation between LCFAs inhibition and presence of double bond structure in LCFAs (Galbraith and Miller, 1973; Kim et al., 2004). It is stated that LCFA inhibition increases with the increase in double bond in LCFAs structure. The hypothesis regarding this concept is that the higher possibility of inhibition of methanogenic microbes due to the presence of an increasing number of double bonds, which provide additional surface area to LCFAs Galbraith and Miller, 1973; Kim et al., 2004). The increase in surface area of LCFAs means that LCFA molecule will interact with methanogenic archaea more consistently. It is also reported that the negative impact of LCFAs towards microbes would increase in the presence of a blend of LCFAs compared to lone LCFA (Koster and Cramer, 1987). There are also few reports claimed that LCFA inhibition is more dominant in the UASB reactor than CSTR due to less dilution effect (J Hunter Long et al., 2012). However, there are still a lot more researches needed to confirm which reactor would be more viable to deal with FOG.

The transient build-up of foam in the digester is another major challenge in anaerobic co-digestion of FOG. Digester foaming happens because of FOG's surfactant property (Husain et al., 2014). The hydrophobic side of the mixture (long carbon chain) accumulates towards the air layer and the polar hydrophilic zone more drawn to the fluid zone, which allows the surface tension to reduce, could trigger foaming in the reactor (Ganidi et al., 2009). Jeganathan et al. (2006) reported that foaming in an up-flow anaerobic sludge blanket reactor (UASB) occurred when FOG loading of 5Kg COD/m³d applied. Few studies reported that an abundance of *Microthrix parvicella*,

filamentous microorganisms in the reactor which trap gas bubble in its hydrophobic filament and creates a foam (Lienen et al., 2014). However, Mullar et al. (2010) mentioned that digester foaming could be controlled by modifying the operating procedure, such as lowering the standpipe of the influent stream.

Another significant operational challenge linked with FOG anaerobic digestion is flotation and washout of sludge (Martín-González et al., 2011). Most of the full-scale anaerobic digesters are operated in CSTR configuration (J Hunter Long et al., 2012). CSTR system has the same hydraulic and solid retention time. Consequently, the sludge floatation effect is minor in the CSTR system. Researchers ascertained the fact that sludge washout effects are more predominant in UASB reactor (Rittman and McCarty., 2001). The efficiency of the UASB reactor is based on the thick sludge bed settled in the reactor where all biological activities take place. To avoid sludge flotation in a UASB reactor, it is recommended to maintain relatively high values of hydraulic retention time (HRT), which provides additional solid retention time for microbes' development in the sludge blanket (Seghezze et al., 1998). Hwu et al. (1998a) observed that the complete flotation occurred at LCFA loading rates above 0.2 g COD/g VSS-d in a continuous UASB treatment process. There are several studies also reported extreme washout of UASB reactors containing lipid-rich wastewater (Salama et al., 2019b). However, M. Madalena Alves et al. (2009) used a flipped anaerobic sludge blanket reactor to extract LCFA from sewage, which facilitates sludge flotation in a manner that could support sludge bed which eventually worked against sludge washout.

Scum deposition in FOG co-digestion is another noticeable concern encountered more often by the WWTP (Salama et al., 2019a). This problem has already been addressed by modifying various operational conditions, such as organic loading rate, proper mixing, thermophilic digestion,

hydraulic retention time, and pH of the stream. It is also suggested that successful feedstock pretreatment can be an alternative way of avoiding scum deposits (Salama et al., 2019a).

2.6 Co-digestion of FOG

Co-digestion provides considerable ecological, technological, operational benefits resulting in enhanced organic waste treatment. Co-digestion is focused on mixing multiple substrates in a proper ratio, which may dilute the inhibitory compound, increase buffer capacity, provide macro-micronutrient equilibrium, create a positive interactive environment for the microbes to grow (Li et al., 2013). Full-scale, pilot-scale, and lab-scale co-digestion of FOG with municipal sewage sludge have been conducted across Europe, the USA, and Canada. Most importantly, co-digestion comes up with enhanced methane yield, which can contribute to achieving better economic feasibility. When considering economic feasibility for industrial-scale application, transport cost of co-substrate to the AD facility also taken into count (Mata-Alvarez et al., 2000). In addition, co-digestion offered a strong usage of land and equipment by digesting completely different waste within the same facility. The results from lab- and pilot-scale studies demonstrated that the addition of FOG causes an increase in the gas production potential of the digester feedstock. This gas production increase, however, may vary drastically depending on the FOG loading, reactor configuration, mixing condition, and possibly other variables. **Table.2.2.** provides a summary of the lab- and pilot-scale FOG anaerobic co-digestion experiments

Table.2.2. FOG co-digestion experiment description

Co-substrate sludge	Experimental design	Control methane production	Maximum methane production	Increase in methane production	Temperature	References
FW	BMP test	60 L/Kg VS	800 L/Kg VS	12 times increase	Mesophilic	(Chowdhury et al., 2019)
PS, WAS	BMP test and Semi continuous	128 ml/ g TVS	400 ml/g TVS	217	Mesophilic	(Kurade et al., 2019)
PS, FW, TWAS	BMP test	130 ml CH ₄ /g TVS	165 ml CH ₄ /g TVS	27	Thermophilic	(Yamrot M Amha et al., 2017)
TWAS	BMP test	316 ml CH ₄	673 ml CH ₄ (Hyper-thermophilic) 492 ml CH ₄ (Thermophilic)	112% (Hyper-thermophilic) 55%(Thermophilic)	Thermophilic and hyper-thermophilic	(Alqaralleh et al., 2016)
SS	Semi continuous (6L reactor)	181 ml/g VS	288 ml/g VS	60%	Mesophilic	(Grosser and Neczaj, 2016)
PS	Semi continuous	-	17.4 L/d (Thermophilic, OLR=2.43 g TVS/L d) 13.1 L/D(Mesophilic, OLR=2.50 G TVS/L d)	-	Mesophilic and thermophilic both	(Li et al., 2013)
SS	Semi continuous	-	700 ml /d	-	Mesophilic	(Martínez et al., 2012)
WAS	Semi continuous-4L	252 L/Kg VS day	598 L/Kg VS day	137	Mesophilic	
KW	BMP test (Thermo chemical pretreated FOG)	258 ml CH ₄ /g TVS added	288 ml CH ₄ /g TVS added	9.9	Mesophilic	(Li et al., 2011a)

WAS	Semi continuous (Thermo alkaline pretreated fatty wastewater)	116 ml CH ₄ /g VS added	362 ml CH ₄ / g VS added	212	Mesophilic	(Carrere et al., 2012)
OFWSW	Semi continuous	N/A	360 ml CH ₄ /g VS a day; Period-1 490 ml CH ₄ /g VS added day; Period -2	-	Thermophilic	(Martín-González et al., 2011)
WAS	BMP test	117 ml CH ₄ /g VS added	418 ml CH ₄ /g VS added	257	Mesophilic	(Li et al., 2011b)
OFWSW	Batch and semi continuous	380 ml CH ₄ /g VS added	550 ml CH ₄ /g VS added		Mesophilic	(Luostarinen et al., 2009)
Sewage Sludge from a WWTP	CSTR (Semi continuous)	278 ml CH ₄ /g VS added	463 L CH ₄ /g VS added	66	Mesophilic	(Luostarinen et al., 2009)
PS and TWAS	Two phase CSTR 1 L – acid phase 4 L – Methane phase	159 (mL CH ₄ /g VS added)	473 (mL CH ₄ /g VS added)	197	Mesophilic	(Kabouris et al., 2009)
PS and TWAS	Two phase CSTR 1 L – acid phase 4 L – methane phase	197 (mL CH ₄ /g VS added)	551 (mL CH ₄ /g VS added)	179	Thermophilic	(Kabouris et al., 2009)
Co-thickened sludge	CSTR	267 (mL CH ₄ /g COD added)	302 (mL CH ₄ /g COD added)	13	Mesophilic	(J. Hunter Long et al., 2012)

Primary and thickened secondary sludge	BMP test	151 mL CH ₄ /g VS added	415 mL CH ₄ /g VS added	175	Mesophilic	(Kabouris,* et al., 2008a)
Primary and thickened secondary sludge	BMP test	143 mL CH ₄ /g VS added	339 mL CH ₄ /g VS added	137	Mesophilic	(Kabouris,* et al., 2008b)
50% WAS 50% PS	BMP test	325 mL CH ₄ /g VS added	681 mL CH ₄ /g VS added	109	Mesophilic	(Luostarinen et al., 2009)
50% WAS 50% PS	CSTR – fed batch	271 mL CH ₄ /g VS added	344 mL CH ₄ /g VS added	27	Mesophilic	(Luostarinen et al., 2009)

BMP-Biochemical methane potential; OFMSW- Organic fraction of municipal solid waste; PS- Primary sludge; WAS- Waste activated sludge; TWAS- Thickened waste activated sludge; KW- Kitchen waste; FW- Food waste

2.7 Role of Microbial community in anaerobic co-digestion of FOG

A complete understanding of the microbial richness and role of LCFA-degrading populations in anaerobic bioreactors is critical towards opening up new methods for the effective treatment of LCFA-rich wastewater. Previous studies have shown the value of biomass adaptation for improved digestion of FOG. However, there have been several reports of biomass inhibition due to LCFA. Initially, most of the research in FOG's anaerobic biodegradation has been based on the process and technological advances, whereas extensive microbiological studies have been limited. More recently researchers are focusing on evaluating microbial community structure and diversity on anaerobic co-digestion of FOG. FOG is a lipid rich material, consequently biodegradation of lipid in anaerobic digestion results in significant higher methane generation due to lipid's high energy potential. Hydrolysis of lipid to glycerol and long chain fatty acids (LCFAs) is known to be very fast process. The rate limiting step in FOG digestion is, conversion of LCFA to methane and carbon-di-oxide. Syntrophic partnerships between desired microbial consortium is key for biodegradation in methanogenic conditions. It is reported that 14 species has the ability to grow with methanogens in syntropy in fatty acid rich wastewater. According to Sousa et al. (2007b) Syntrophic degradation of LCFAs in methanogenic conditions relies on the behavior of hydrogenotrophic microorganisms that ensure low hydrogen concentration in the bioreactor. Also, acetoclastic methanogens play an important in conversion of LCFA to methane as acetate-derived methane accounts for nearly 70% of LCFA's total theoretical methane capacity. Study suggested that LCFA might have toxic effect on acetolactic methanogen. However, Pereira et al. (2005) stated that the decline in methanogenic activity is temporary and also described that with the course of time, methanogenic activity increases which resulted in efficient conversion of LCFA to methane. In a study conducted by Sousa et al. (2007a) reported that in the batch degradation of

oleate and palmitate, methanogenic archaea increased by $85 \pm 29\%$ and $75 \pm 14\%$, respectively. Alves et al. (2001) and Silva et al. (2014) suggested that biomass resistance towards LCFA is influenced by the time of exposure to lipids. Ziels et al. (2016). Silvestree et al. (2011) investigated that gradual increase in FOG loading induced higher rates of beta-oxidation and methanogenesis. Ziels et al. (2016) also found that substantial growth of LCFA degrading biomass and methanogenic archaea in the FOG co-digester with time being. This study reported syntrophic beta-oxidizing genus *Syntrophomonas* increased to approximately 15% of the digester bacteria population, and *Methanosaeta* and *Methanospirillum* were found to be the most dominant archaea, comprised almost 80% of total archaeal community. The *Syntrophomonadaceae* family was previously identified as a syntrophic bacteria group responsible for degradation of unsaturated fatty acids whereas *Syntrophaceae* is found in higher abundances in saturated LCFA degrading anaerobic populations. Amha et al. (2017) also confirmed about positive correlation of methane production with LCFA degrading biomass. All these findings potentially suggest that it is possible to achieve more effective LCFA conversion into methane by efficiently controlling intermittent FOG loadings to provide sufficient time for microbial population adaptation by enrichment of higher LCFA-degrading consortia

2.8 Application of conductive additives in anaerobic digestion

In anaerobic digestion, methane is produced through metabolic activity of acetoclastic and hydrogenotrophic methanogens which utilize acetate and H_2/CO_2 , respectively. The mechanism of electron transfer in the form of hydrogen between syntrophs (i.e., fermentative bacteria) and methanogens is called as interspecies hydrogen transfer (IHT) (Yang et al., 2017a). This mechanism of electron transfer to form intermediate metabolites is considered as less efficient (Lin et al., 2018b). There are several kinetic limitations associated with IHT kinetics, firstly diffusion of H_2 from producers to methanogens is very slow (Liu et al., 2012). Secondly, H^+ as an electron acceptor in AD is less competent because of its weak oxidative-reductive ability ($H^+/H_2 = -414$ mV), and this process is also thermodynamically unfavorable, which leads to slow electron transfer (Yang et al., 2017a). The slow electron exchange rate among the target anaerobes is one of the main reasons that lower the efficiency of AD. As IHT is thermodynamically not feasible, lowering H_2 concentration can be an alternative solution to make this process thermodynamically feasible. To lower H_2 concentration, there needs to be sufficient enrichment of hydrogenotrophic methanogens that consume H_2 to form methane (Wang et al., 2018). However, several reports suggested that H_2 -consuming methanogens are usually not dominant in conventional anaerobic digesters (Yang et al., 2017b). Therefore, to address these challenges more thermodynamically feasible solution is needed.

Direct interspecies electron transfer (DIET) is a recently discovered microbial electron transfer process that enables some syntrophic bacteria to pass electrons directly to methanogens instead of H_2 interspecies transfer (Zhao et al., 2017a). In DIET, some bacteria form an electrical connection with their syntrophic partners (e.g., methanogens) by producing conductive nanowires (Yang et al., 2017b). Moreover, the addition of various conductive materials could promote DIET between

syntrophic partners (Zhao et al., 2017a). Granular activated carbon (GAC), biochar, carbon cloth, magnetite all these materials found to have the ability to promote DIET within a variety of bacteria that are unable to produce conductive nanowires (Barua and Dhar, 2017). The conductive materials work more as a bridge to carry electrons to desired microbes. Therefore, microbes don't have to invest their energy in forming conductive pili. Thus, DIET allows methane production in a thermodynamically and metabolically favorable manner and thereby enhancing methane production rates and yields.

Studies have already shown that electron recovery from reduced organic compounds as methane is more significant via DIET (Dang et al., 2016; Liu et al., 2012; Zhao et al., 2015). Few studies also reported that addition of GAC and Magnetite in bioreactor certainly minimize VFA accumulation, and these materials can also deal with high organic loading AD system (Barua and Dhar, 2017). To date, most of the studies with conductive materials to promote DIET in anaerobic digestion system are limited with model substrates such as ethanol, acetate, propionate butyrate. To promote DIET, GAC has been frequently used in both continuous and semi-continuous reactor. It was evident from the previous studies that GAC amended reactor showed superior methanogenesis kinetics compared to control digester while utilizing ethanol, acetate, propionate, butyrate, dog food, etc. (Zhao et al., 2017a). GAC amended reactor performed better compared to control, possibly due to GAC attached biomass formed thick and stable biofilm due to larger surface area (m^2/L) (Wang et al., 2018). Another conductive material that has been well confirmed to promote DIET in anaerobic digesters is magnetite nanoparticles. However, the mechanism of magnetite in promoting DIET is different from other conductive material due to its surface property (Cruz Viggi et al., 2014). The main difference is in case of granular conductive materials microbes choose granule as their electron exchange medium whereas iron nanoparticles, it attaches

with conductive pili of microbes to transfer electron (Wang et al., 2018). Thus, with magnetite, promoting DIET could be complex due to significant interspecies distances between microbes and less availability of microbes having conductive pili in their formation. However, to date limited information is available in the literature on how the conductive materials like GAC and magnetite can influence the co-digestion of real organic wastes such as FOG and FW combination. Therefore, the addition of these conductive materials in the co-digestion of FOG and FW may reveal an improved pathway to achieve bioenergy from these complex wastes.

Chapter 3

Materials and Methods

3.1 Substrate and inoculum

The FW and FOG samples were collected from a student residence (University of Alberta, Edmonton, AB, Canada), and a poultry industry (Southwestern Ontario, Canada), respectively. Upon receipt, the food waste was properly blended using an electric mixer. Digester sludge collected from a full-scale sewage sludge digester (Gold Bar Wastewater Treatment Plant, Edmonton, Alberta) was used as the inoculum. All the materials were stored at 4 °C before use. Prior to experiment, the inoculum was acclimated at 37 °C for 3 d. The average characteristics of FW are as follows: total chemical oxygen demand (TCOD): 288298±13157 mg L⁻¹, soluble chemical oxygen demand (SCOD): 44438±2495 mg L⁻¹, total solids (TS): 192000±2803 mg kg⁻¹, volatile solids (VS): 174783±3276 mg L⁻¹, total ammonia nitrogen (TAN): 324±3 mg L⁻¹, pH: 5.15. The average characteristics of FOG are as follows: TCOD: 438777±9395 mg L⁻¹, SCOD: 41904±566 mg L⁻¹, TS: 229949±11105 mg L⁻¹, VS: 222813±10743 mg L⁻¹, TAN: 1618±65 mg L⁻¹, pH: 6.74.

3.2 Experimental design

In phase-1, biochemical methane potential (BMP) test was conducted using different ratios of FW and FOG based on wet weight: 90% FW + 10% FOG, 80% FW + 20% FOG, 70% FW + 30% FOG, and 60% FW + 40% FOG. Two additional control experiments were performed with 100% FW and 100% FOG. Food (COD of co-substrates) to microorganism (VS of anaerobic digester sludge) (F/M) ratio was 1.5 (g-COD of substrate/g-VS of inoculum). Sodium bicarbonate (6 g L⁻¹) was added as additional buffer. The initial pH of the materials was in the range of 7–7.5.

In phase-2, co-digestion at the optimum mixing ratio of FOG and FW from phase-1 was further investigated with the addition of different conductive additives: GAC (25 g L⁻¹) and magnetite (25 mM as Fe) (Barua and Dhar, 2017). Before use, GAC (8-20 mesh; Sigma-Aldrich, Canada) was thoroughly washed with de-ionized water and then dried at 105 °C. Magnetite particles (95% pure, powder size < 5 µm; Sigma Aldrich, Canada) was directly used. Digested sludge from the optimum co-digestion condition in phase-1 was further used as the inoculum for phase-2. In phase-2, BMP test were conducted in multiple fed-batch cycles and the duration of each cycle was 20 d. In the first cycle, the F/M ratio was 1.5. In the following cycles, 55 mL of digested sludge was replaced with fresh feedstock at the optimum mixing ratio of FOG and FW from phase 1. Before feeding, mixing was stopped and given 2 h of settling time.

All bioreactors were purged with N₂ gas for about 3 min to create an anaerobic environment. Each reactor was assembled with a mechanical agitator plus an electric motor (ISES-Canada, Vaughan, ON, Canada) for continuous mixing at 300 rpm during experiment. All experiments were conducted at mesophilic condition (37±2°C) using water baths. All the experiments were conducted in triplicate.

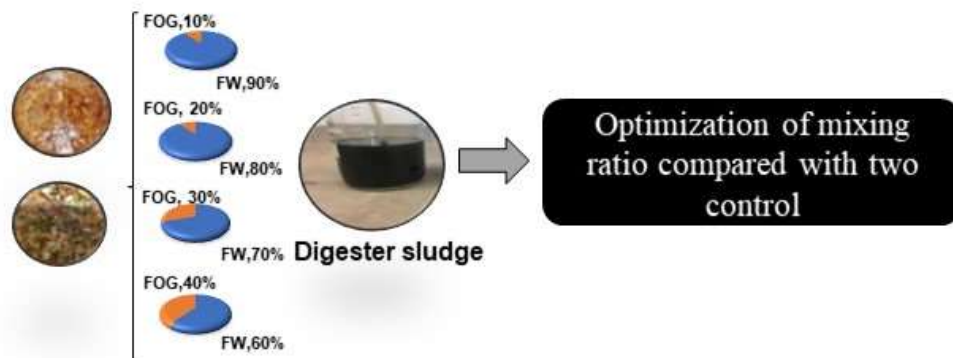


Figure 3.1. Experimental design of optimization of co-digestion of FOG and FW

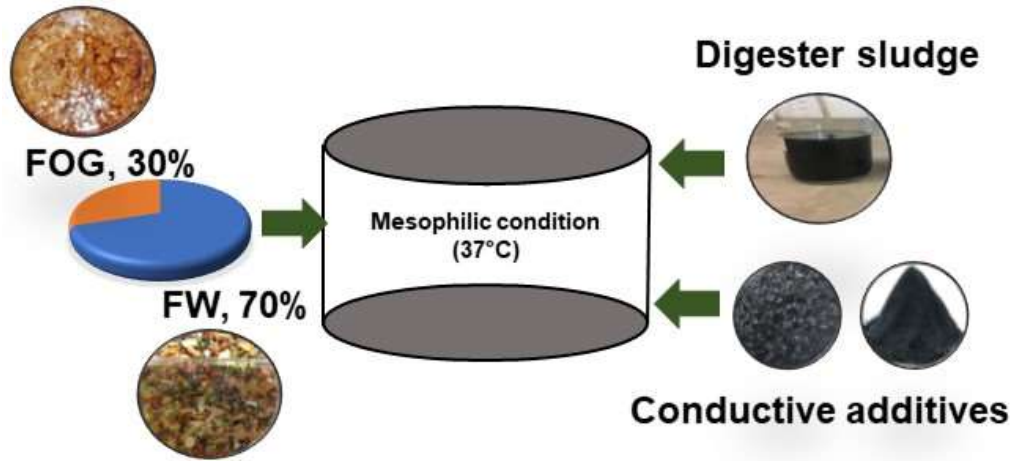


Figure 3.2. Experimental design of addition of conductive materials in co-digestion of FOG and FW



Figure 3.3. Overhead view of BMP test.

3.3 Analytical methods

TCOD, SCOD, TAN concentrations were analyzed using HACH reagent kit (HACH, Loveland, CO, USA). Samples used for the analysis of SCOD and TAN were prepared by centrifugation at

8000 rpm for 5 min followed by filtering with 0.45 μm filter. VFAs (Acetate, Propionate, Butyrate) samples after filtering (0.20 μm) were analyzed with an ion chromatograph (DionexTM ICS-2100, Thermo Scientific, USA) equipped with an electrochemical detector (ECD) and microbore AS19, 2 mm column. The operating temperature of the column was 30 °C and conductive detector temperature was set at 35 °C. The eluent was 7.00 mM KOH and the eluent flow rate was 0.25 mL min^{-1} using an eluent generator (EGC II KOH, Thermo Scientific). The volume of produced methane was collected using gas bags connected with CO₂ absorption unit; 3M NaOH solution with thymolphthalein indicator was used to absorb the CO₂ from biogas (Ryue et al., 2019). Methane volume was manually measured using a gas syringe on a daily basis and reported per gram of initial VS of substrates added to the bioreactor.

Fourier transform infrared spectroscopy (FTIR) analysis was conducted for raw substrates and the final effluent after the completion of 5th cycle of co-digestion test with conductive additives. Samples were dried at 105 °C for 48 h, and then 2 mg of samples were ground up with 200 mg of KBr (FTIR Grade) in an agate mortar to make the sample homogenized. Infrared spectra for the samples were measured over the range of 4000-400 cm^{-1} at a rate of 0.5 cm^{-1} using an FTIR Perkin-Elmer 2000 spectrophotometer. Fifty scans were obtained for each spectrum and all the data were corrected against air as background. All the samples were analyzed in triplicate and the average values were reported.

3.4 Modeling and statistical analyses

Ideally, the lag phase and methane production can be assumed by conventional first order rate kinetics. However, for better understanding the cumulative methane production rate over the time non-linear regression has been in many studies used. The modified Gompertz model is actually modification of first order rate kinetics. The modified Gompertz model was used to predict the

methane potential, the maximum methane production rate, and lag phase as described in Eq. 1 (Das and Mondal, 2015).

$$H(t) = H_{max} \times \exp \left\{ - \exp \left[\frac{R_{max} \times e}{H_{max}} (\lambda - t) + 1 \right] \right\} \quad (\text{Eq. 1})$$

Where $H(t)$ is cumulative methane production (L kg VS^{-1}) at time t ; H_{max} is methane potential (L kg VS^{-1}); R_{max} is maximum methane production rate (L kg VS-d); λ is time of lag phase (d). Average results and standard errors were reported based on triplicate for each treatment. Statistical significance was tested using analysis of variance (ANOVA) and student's t test in R project (v.3.5.1) with a threshold p -value of 0.05. Principle component analysis (PCA) was performed to further analyze the FTIR spectral data sets using The Unscrambler X (Evaluation version 10.5) software.

3.5 Microbial community analysis

After the completion of 5th cycle, biomass samples collected from the control, magnetite and GAC amended bioreactors were characterized with high throughput 16S rRNA gene sequencing. For control and magnetite amended reactors, suspended biomass was collected. For GAC amended reactors, both suspended and GAC attached biomass were collected for DNA extraction. Total metagenomic DNA of the biomass samples were extracted using PowerSoil[®] DNA Isolation Kit (MoBio Laboratories, Carlsbad, CA, USA). The DNA concentrations and quality were determined using a spectrophotometer (NanoDrop 2000C, Thermo Fisher Scientific, Waltham, MA, USA). The extracted DNA samples were stored immediately at -70 °C prior to 16S rRNA gene sequencing (Research and Testing Laboratory, Lubbock, TX, USA) using the universal primer set 515F/805R to target the V3-V4 region of 16S rRNA gene. The software Quantitative Insights Into Microbial Ecology (QIIME v2) was used to analyze the demultiplexed sequencing data (Caporaso

et al., 2010). The sequences were first processed to denoise and join paired-end reads (DADA2 method) (Callahan et al., 2016). The denoised sequences were assigned to species-equivalent operational taxonomic units (OTUs) at a 97% sequence similarity level using the open-reference OTU picking method (VSEARCH method against 2013-08 Greengenes database) (Rideout et al., 2014). Bacterial and archaeal quantity in the DNA samples were evaluated by real-time quantitative PCR (qPCR) analysis.

Chapter 4

Results and Discussion

4.1 Optimization of mixing ratios of FW and FOG

Fig.4.1 shows the cumulative methane production at different mixing ratios of FW and FOG. The experiments were conducted for 50 d until most of the reactors stopped producing methane. The bioreactor with 100% FOG had the most extended lag phase (30 d) and lowest methane production ($67 \text{ L CH}_4 \text{ kg VS}^{-1}$), possibly due to the inhibition of LCFA. After 30 d, its methane production rate increased slightly, indicating that the inhibition caused by LCFAs could be reversible when microbes started to degrade LCFAs after a lag phase. Generally, LCFA conversion to methane considered as the rate limiting steps in FOG digestion (Yamrot M. Amha et al., 2017); thus a longer lag phase with FOG was expected.

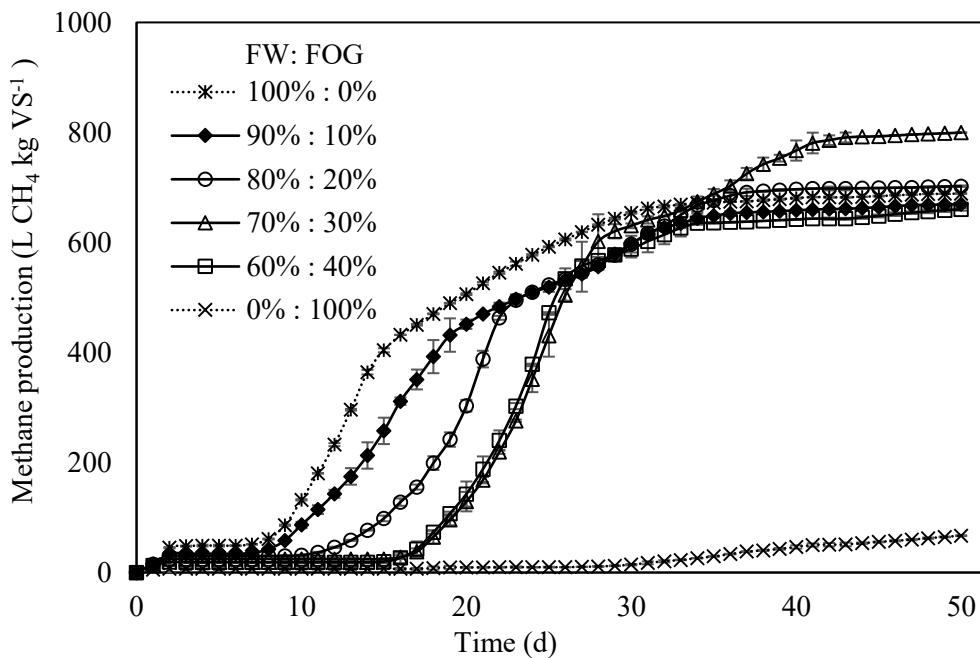


Fig. 4.1. Methane production at different mixing ratios of FW and FOG.

In contrast, the bioreactor with 100% FW had the shortest lag phase (8 d) with a methane production of 689 L CH₄ kg VS⁻¹. As the FW portion decreased from 100% to 60%, the lag phase gradually prolonged from 8 to 15 d. With the increase of FOG portion from 10% to 30%, methane production increased from 669 L CH₄ kg VS⁻¹ to 800 L CH₄ kg VS⁻¹, but with a further increase of FOG to 40%, methane production decreased to 660 L CH₄ kg VS⁻¹, indicating the fact that higher FOG loading could inhibit methane production, which were in line with previous studies (Wu et al., 2018; Xu et al., 2015a). The optimal methane production (800 L CH₄ kg VS⁻¹) was obtained from 70% FW+ 30% FOG, which was 1.2 times and 12 times of that obtained from 100% FW and 100% FOG, respectively. Two recent studies investigated co-digestion of FW and FOG in semi-continuous mode under mesophilic condition and found optimal methane production of 740–810 ml CH₄ g VS⁻¹_{added} (Wu et al., 2018; Xu et al., 2015a), which were comparable to the values obtained in this study.

These results demonstrated synergistic effects of co-digestion of FW and FOG on methane production. It is also noticeable that all reactors with FW started to reach a plateau for methane production after 30 d. Interestingly, 70% FW+30% FOG combination showed dual phases of exponential methane production; 15-30 d and 30-40 d. This could be attributed to that FW was readily degradable, contributing to the first phase of methane production; after 30 d, FOG mainly contributed to the second phase of methane production due to slower degradation of LCFAs. The dual-phase phenomenon of methane production was also observed in co-digestion with other mixing ratios, but to different degrees.

4.2 Impact of conductive additives on co-digestion performance

4.2.1 Methanogenesis kinetics

Fig.4.2 shows the effect of conductive additives on co-digestion of FW and FOG in five consecutive fed-batch cycles. The optimal ratio of 70% FW+30% FOG was used as the control. In cycle-1, control bioreactor showed the longest lag phase (10 d), followed by bioreactors with magnetite (8 d) and GAC (6 d). While their cumulative methane productions were comparable (663-720 L CH₄ kg VS⁻¹).

Meanwhile, control bioreactor showed shortened lag phase as compared to phase-1 (20 d vs. 10 d) due to the acclimation of inoculum. In cycle-2, GAC-amended reactor started to produce methane with minimal lag phase of only 4 d and reached a plateau after 10 d, achieving a significantly ($p<0.05$) higher total methane production (702 L CH₄ kg VS⁻¹) than those from the other two reactors (390 L CH₄ kg VS⁻¹-610 L CH₄ kg VS⁻¹). Notably, both control and magnetite reactors showed inferior performance, which suggested that there might be imbalance between acidogenesis and methanogenesis kinetics. In cycle-3, all reactors showed shorter lag phases than cycle-2, suggesting acclimation of the microbiome. GAC supplemented reactor immediately started to produce methane. Both magnetite and control reactors reduced lag phases to 6 d compared with previous cycles. In cycle-4 & 5, GAC reactor showed repetitive performance as previous cycles. While magnetite and control reactors showed comparable performance to each other, both further shortened lag phases (from 6-7 d to 4-5 d) and the time to reach plateau for methane production (from 20 d to 12 d) compared to cycle-3.

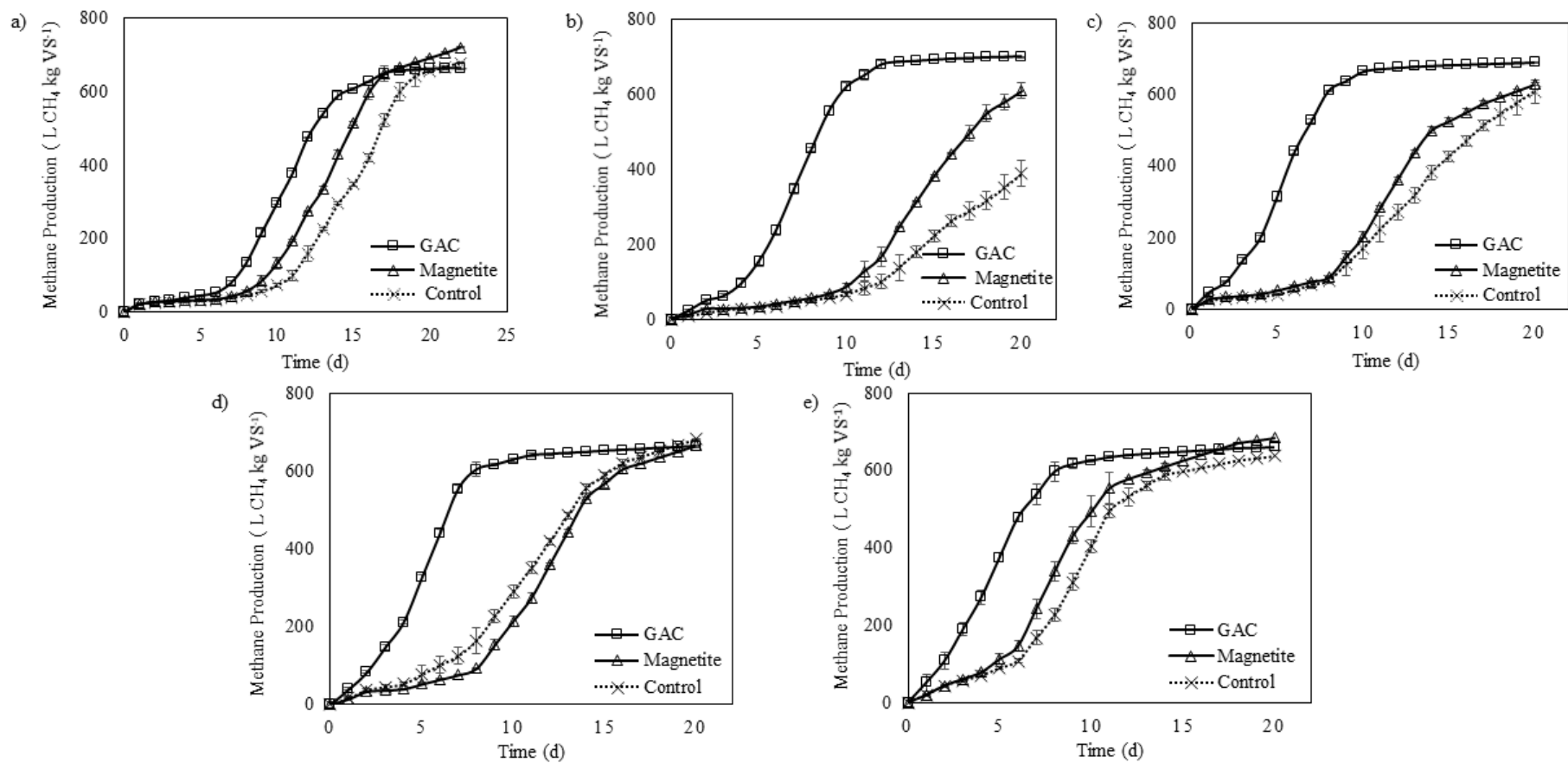


Fig. 4.2. Effect of different conductive additives on co-digestion of FW and FOG. Note. Control indicate co-digestion (70% FW+30%FOG) without any conductive additives. (a)-(e): Cycle-1 to cycle-5.

Table.4.1 shows the average results of fitting modified Gompertz model to 5 cycles of experimental methane production data. The detailed modeling results of fitting Gompertz model for each cycle are provided in the Supplementary Information. The values of methane potential, maximum methane production rate, and lag phase estimated for control and magnetite reactors were comparable ($p>0.05$). With GAC addition, the maximum methane production rate (108 L/kg VS-d) increased by 50-80% compared to other two reactors (60-72 L/kg VS-d). The lag phase was also significantly shortened from over 7 d to 3 d with addition of GAC. Collectively, GAC addition profoundly reduced the lag phase and improved the methane production rate during co-digestion of FW and FOG, which were in line with some other studies reported enhanced mono-digestion complex feedstocks in GAC-amended digesters (Yang et al., 2017b; Zhao et al., 2015). However, researchers have also studied the impact of magnetite on methanogenesis with positive outcomes, but they focused mainly on simple organic substrates (i.e. ethanol, acetate, propionate, etc.) (Barua and Dhar, 2017; Cruz Viggi et al., 2014). However, there are limited studies on the application of magnetite in anaerobic digestion of complex substrates such as FW and FOG. The complex of FW and FOG could limit the function of magnetite. For instance, lipid could adsorb around the biomass and magnetite surface, limiting the contact of microbes (J. Hunter Long et al., 2012).

Table.4.1. Results for modified Gompertz model fitting (average of 5 cycles).

Condition	Modified Gompertz model			
	CH ₄ potential (L kg VS ⁻¹)	Maximum CH ₄ production rate (L/kg VS ⁻¹ -d ⁻¹)	Lag phase (d)	R ²
Control	960 ± 355	60 ± 13	7.4 ± 3	0.994
Magnetite	762 ± 91	72 ± 9	6.9 ± 2	0.994
GAC	684 ± 22	108 ± 11	3.0 ± 2	0.996

4.3 VFA accumulation

Fig. 4.3(a) shows concentrations of VFAs (i.e. acetate, propionate, and butyrate) after completion of cycle-5. Obviously, control showed the highest VFA concentrations followed by bioreactor amended with magnetite and GAC. The acetate (865 mg COD L⁻¹ vs 247–93 mg COD L⁻¹), propionate (1532 mg COD L⁻¹ vs 34–12 mg COD L⁻¹) and butyrate (118 mg COD L⁻¹ vs 56–32 mg COD L⁻¹) in control were 3.5-9.3, 45-127, 2.1-3.7 times of those in magnetite and GAC bioreactors, respectively. Interestingly, magnetite amended reactor showed significantly lower final VFA concentrations than control, although ultimate methane productivities were comparable. Nonetheless, the results clearly showed that GAC addition could alleviate the accumulation of these three VFAs specially propionate which is often found to be the most robust organics for the conversion of methane (Stams and Plugge, 2009). Conversion of propionate is correlated with the partial pressure of hydrogen, which requires the hydrogen partial pressure to be below 10^{-4} atm (Siriwongrungronson et al., 2007). Thus, the significantly lower levels of propionate in both magnetite and GAC reactors might be likely due to enrichment of hydrogen utilizing methanogens.

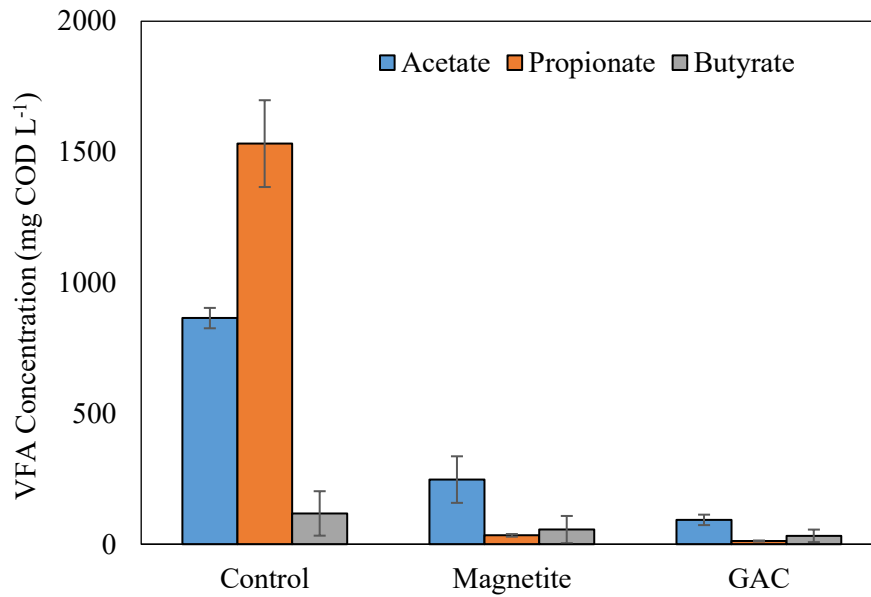


Fig. 4.3. Accumulation of VFAs concentration from cycle-5.

4.4 Ammonia nitrogen

Ammonia concentration in anaerobic digestion and co-digestion is very vital to maintain process stability. Proper ammonia concentration in the reactor provides buffering capacity for maintaining microbial activity. However, high ammonia level could inhibit methanogenesis, resulting in potential digester failure (Rajagopal et al., 2013). Fig. 4.4 (b) shows the initial and final ammonia concentrations from three reactors for cycle-5. Initial ammonia concentration for control, magnetite and GAC reactors were 2579, 3135 and 2734 mg L⁻¹, respectively. After cycle-5, ammonia concentration slightly increased by 6% in control reactor, but decreased by 13.5% and 7.5% in the reactors amended with GAC and magnetite, respectively. This might be attributed to adsorption of some ammonia by magnetite and GAC in their micro pores (Florentino et al., 2019). The reported inhibitory ammonia levels ranged widely (1500-7000 mg L⁻¹) in literature depending on the substrate characteristics (Rajagopal et al., 2013; Wu et al., 2018). The values observed in this study were ~40% higher than those reported in a previous study on anaerobic digestion of FW

(Ryue et al., 2019). Although the final ammonia concentrations of all the reactors were in the inhibitory range but methane production was stable throughout the cycle-5. As discussed later, *Methanosarcina* spp. were the most dominant methanogens in all the three bioreactors in this study, which was also consistent with previous reports on their higher tolerance against ammonia (Karakashev et al., 2005).

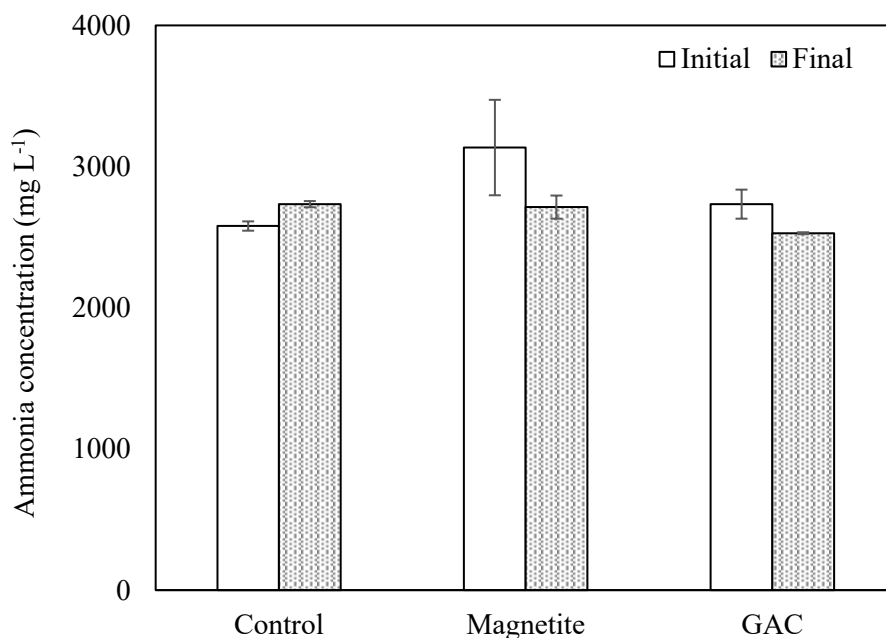


Fig 4.4. Initial and final ammonia concentration from cycle-5.

4.5 FTIR results

The chemical structures and functional groups of initial substrates and final digestates were also characterized using FTIR spectroscopy to assess their degradation (Kataki et al., 2017). The FTIR spectra of the initial substrates and final digestates are illustrated in Fig. 4.5.(a) FW exhibits a broader and higher absorbance than FOG around 3400–3300 cm⁻¹ (Fig. 4a), which is ascribed to O-H vibration of carboxylic and alcoholic groups, as well as to amide hydrogen vibrations (Cuetos et al., 2009; Martínez et al., 2012). The results suggest rich contents of carboxylic acids, alcohols,

and/or protein in FW. In contrast, FOG shows stronger peaks between 2800-2930 cm^{-1} than FW, which are attributed to the aliphatic C-H stretching (Castaldi et al., 2005), indicating a higher aliphatic degree and lipid content in FOG. On the other hand, the absorption peaks between 1700-1750 cm^{-1} associate with the vibration of carbonyl group (C=O), which suggests the presence of aldehyde, ketone, ester, protein, or carboxylic acid compounds (Cuetos et al., 2009; Hafidi et al., 2005; Meissl et al., 2007). Moreover, relatively high absorption bands are observed for FW around 1200-1100 cm^{-1} (C-N functional group) and 1033 cm^{-1} (vibration in carbohydrates, aromatic ethers and polysaccharides) (Cuetos et al., 2009; Spaccini and Piccolo, 2008), which also supports the high protein content and readily available organic matter in FW.

Fig. 4.5.(b) showed FTIR spectra of final samples from control, magnetite and GAC amended reactors. Notably, the absorbance peaks are the most intense for control, followed by magnetite and GAC amended reactors. Compared to the original substrates, the characteristic bands associated with lipids and fats, such as C-H stretching in the range of 2800 and 3000 cm^{-1} , were greatly reduced in all the final digested samples. The results demonstrated remarkable decrease in aliphatic structures after five cycles of operation (Cuetos et al., 2009). The decrease in the absorbance at 1700-1750 cm^{-1} also indicates the degradation of esters, protein, and/or volatile compounds. Accordingly, the high peaks around 1460–1380 cm^{-1} are assigned to aliphatic C–H deformation, O–H deformation, C=O stretching of phenols, and anti-symmetric COO– stretching (Cuetos et al., 2009). These strong peaks along with the presence of absorbance intensity associated with O-H vibration of carboxylic and alcoholic groups (3300-3500 cm^{-1}) also support the degradation of lipids and existence of intermediates in all the final samples. Moreover, the intense peaks near $\sim 1000 \text{ cm}^{-1}$ (vibration in carbohydrates, aromatic ethers and polysaccharides) demonstrated incomplete digestion of the organic matter in all the three reactors, which is the most

profound in control reactor (Spaccini and Piccolo, 2008). On the other hand, when readily degradable organics are degraded, the degree of aromaticity increases. The intense absorbance at around 1640-1620 cm^{-1} (stretching of C=C in aromatic groups) implies microbial decomposition of wastes and formation of certain aromatic compounds (Cuetos et al., 2009). Overall, the results suggest degradation of lipids, protein and carbohydrates to some degree and existence of intermediates in all the three reactors, showing a decreasing trend in most of the functional group peaks in GAC, magnetite and control reactors.

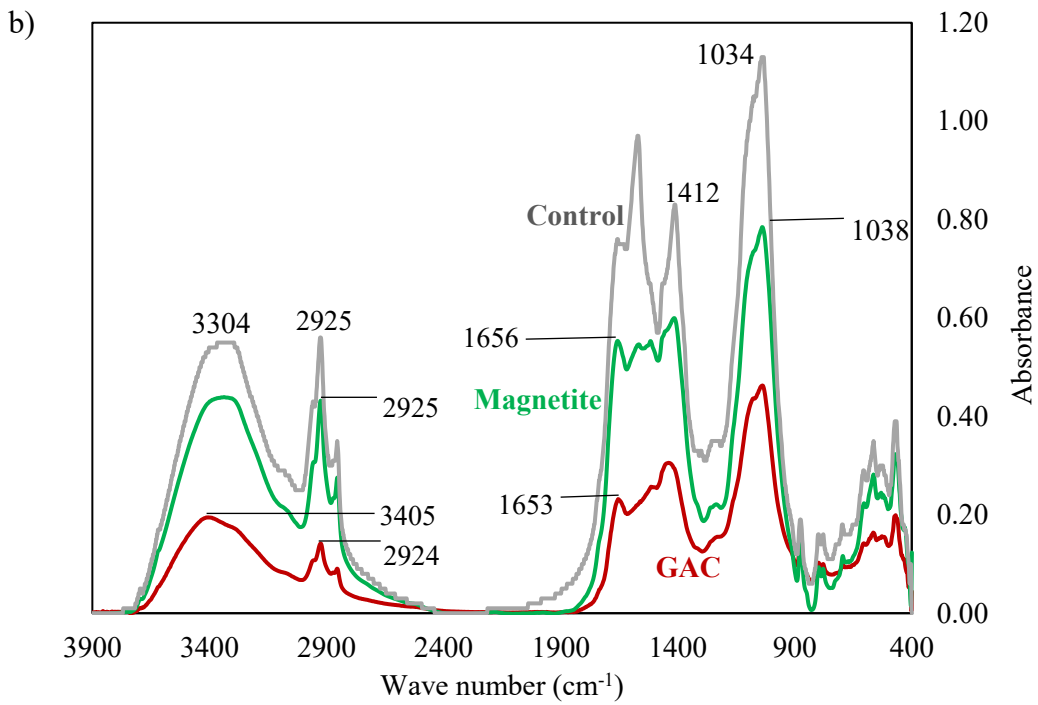
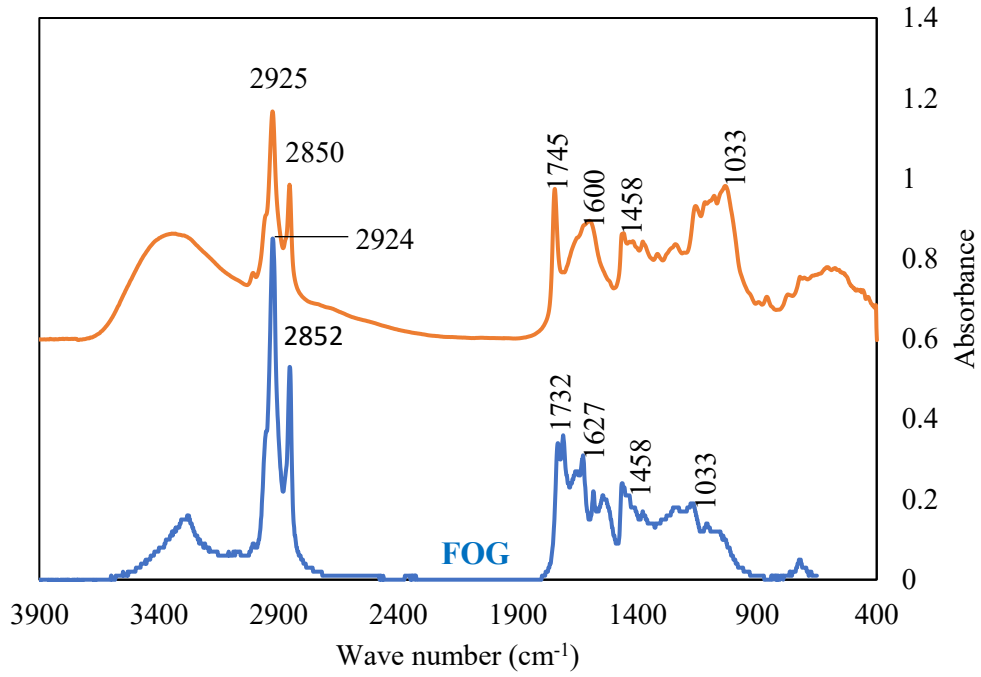


Fig 4.5. FTIR spectrum of (a) FW and FOG, and (b) final digestate.

The application of PCA to the spectral profiles of FOG, FW and final digestates is shown in Fig. 5. The PC1 (89%) and PC2 (7%) together explain 96% of the total variations (Fig. 4.6.(a)). The two initial substrates (FOG and FW) are clearly distinct from the three final digestate samples (GAC, magnetite, and control) along both PC1 and PC2. The loading of PC1 is mainly contributed by a broad peak at 3300 cm^{-1} (carboxylic and alcoholic groups) and high peaks at $1400\text{-}1700\text{ cm}^{-1}$ (carbonyl group (C=O); aliphatic C-H deformation; C=C in aromatic groups) and 1000 cm^{-1} (polysaccharides) (Fig. 4.6.(b)). These peaks mainly originate from absorption bands of intermediates such as polysaccharides, carboxylic acids and alcohols (Cuetos et al., 2009; Hafidi et al., 2005; Martínez et al., 2012; Meissl et al., 2007; Spaccini and Piccolo, 2008). Samples from control and magnetite reactor both have a positive score on PC1, correlating with high peaks in these regions. Thus, the separation along PC1 is dominated by the content of intermediates in samples. In contrast, the loading of PC2 is mainly due to the variation in the spectral regions centered at 2900 cm^{-1} (aliphatic C-H stretching) and 1700 cm^{-1} (carbonyl group), corresponding to lipid, protein and/or carboxylic acids compounds (Castaldi et al., 2005; Cuetos et al., 2009; Hafidi et al., 2005; Meissl et al., 2007). Minor contributions of bands at 1000 cm^{-1} are also observed. Samples of FOG, FW and control reactor have a negative score on PC2, correlating with high peaks in these regions. Thus, the separation along PC2 is dominated by the contents of lipid, protein, and carbohydrate. The intermediate contents are inversely correlated with lipid and protein contents as seen from opposing peaks in the loading plot (Fig. 4.6(b)). Furthermore, the score plot shows that the sample from GAC reactor is distinctly different from other samples, in a region implying low contents of lipid and intermediates. The PCA plots further supported the significant difference of the final digestate from the three reactors.

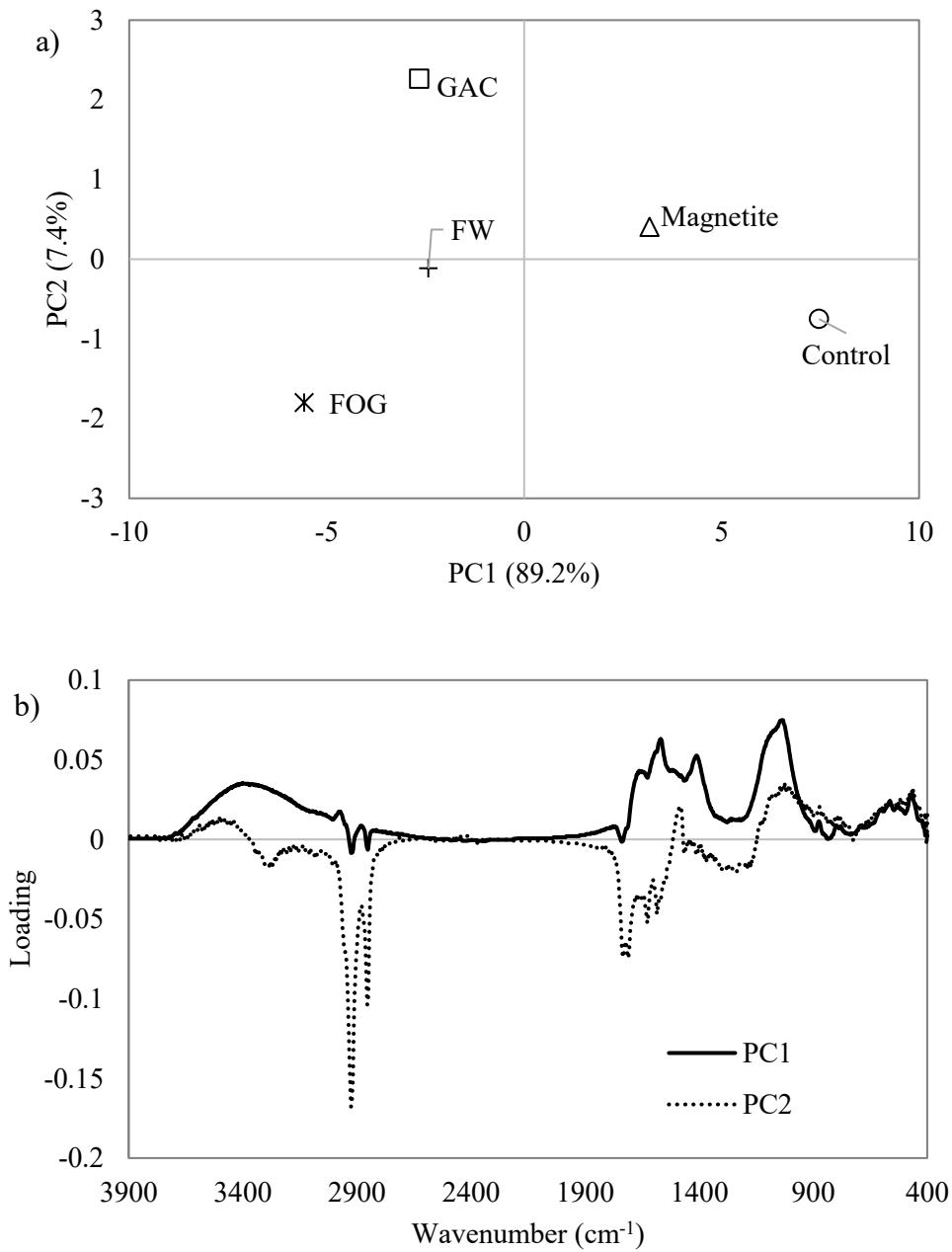


Fig 4.6. Principal component analysis for FTIR spectroscopy results (a) score plot and (b) loading plot of PC1 and PC2 from PCA.

4.6 Microbial community

4.6.1 Quantitative analysis of microbial population

The quantitative analysis of microbial biomass was performed to attain further insights into the differences in methane production rates from different reactors (Table 2). The qPCR results showed that the amounts of both bacterial and archaeal cells were substantially higher (1-2 orders of magnitude) in GAC and magnetite amended reactors compared to control (bacteria: 1.8×10^8 cells mL⁻¹, archaea: 3.0×10^7 cells mL⁻¹). Notably, for GAC amended reactor, microbial cells were more concentrated in GAC surface (bacteria: 3.5×10^9 cells g⁻¹ GAC, archaea: 1.3×10^9 cells g⁻¹ GAC) over suspended sludge (bacteria: 7.7×10^8 cells mL⁻¹, archaea: 1.8×10^7 cells mL⁻¹). Thus, GAC appeared to be more advantageous in extending the biomass retention in this study.

Additionally, the relative abundances of archaea in the prokaryotic community (both archaea and bacteria) were also shown in Table 2. Interestingly, the fraction was the highest in GAC attached sample (27%), followed by control (14%), magnetite (9.7%) bioreactors, and GAC suspended sample (2.3%). Moreover, in the GAC-amended reactor, the major portion of archaea (64%) was attached to GAC surface, while most of the bacteria (90%) were suspended in bulk sludge. It was evident that the addition of conductive materials greatly increased total microbial cell numbers in this study. This finding was different from a previous study that use acetate as the carbon source (Zhang et al., 2017), in which addition of GAC did not result in an increase of microbial biomass. The difference could be attributed to different substrates: with simple substrates, the collision and friction among granular particles could make the biofilm hard to form (Zhang et al., 2017); while using complex substrates, especially greasy materials like FOG and FW, substrates could adsorb around GAC surface preventing the biofilm on GAC surface from collision and friction during operation.

4.6.2 Microbial diversity

Alpha diversity indices were also calculated to compare the microbial community diversity among three bioreactors (Table 4.2.). Results showed that both microbial richness (OTUs and Chao1) and diversity indices (phylogenetic distance and Shannon) tended to be higher in magnetite and GAC amended reactors compared to control, indicating a higher microbial richness and diversity due to the addition of magnetite and GAC. Furthermore, GAC attached sample showed the highest microbial richness (Chao1: 176) and diversity indices (Shannon: 5.65) among all samples, which has also been reported previously on food waste digestion with GAC addition (Ryue et al., 2019). These results suggested that the presence of GAC and magnetite can not only increase microbial abundance, but also enhance microbial richness and diversity; the enhancement was to a larger degree in GAC compared to magnetite.

Table 4.2. Total microbial abundance and diversity indices from three bioreactors.

Sample	Microbial abundance			Microbial diversity indices			
	Archaea (16S copies/mL sample)	Bacteria (16S copies/mL sample)	Relative abundance of Archaea, %	OTUs	Chao1	Phylogenetic distance	Shannon
Control	3.02×10^7	1.83×10^8	14.2%	51	51	7.13	4.66
Magnetite GAC attached	4.24×10^7	3.93×10^8	9.7%	72	72	9.46	4.60
GAC suspended	1.28×10^{9a}	3.47×10^{9a}	27.1%	174	176	17.74	5.65
	1.77×10^7	7.69×10^8	2.3%	141	148	14.67	4.22

Note: ^aBased on g of GAC (16S copies/g GAC)

4.6.3 Bacterial and archaeal community

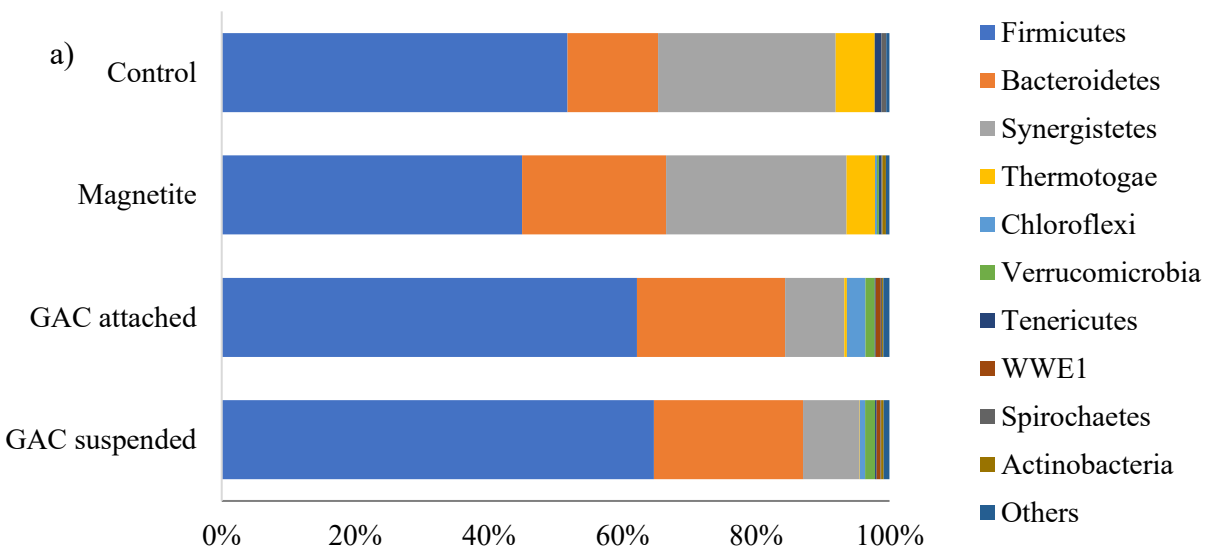
Fig. 4.7.(a) shows the relative abundance of bacterial community at the phylum level. The three most predominant phyla were *Firmicutes*, *Bacteroidetes*, and *Synergistetes* (together >90%) in all reactors. With GAC addition, the relative abundance of *Firmicutes* increased (64% vs. 45-52%) while *Synergistetes* (8% vs 26.6-27.1%) decreased compared to control and magnetite amended reactors. *Bacteroidetes* was comparable in relative abundance in GAC and magnetite amended reactor (22%), which was slightly lower in control (14%). Considering microbial abundance, all these three phyla increased by 1-2 orders of magnitude with GAC and magnetite addition. *Firmicutes* contains various fatty acid- β -oxidizing bacteria, while some *Bacteroidetes* members are known as proteolytic bacteria (Lin et al., 2017; Ziels et al., 2016). Nonetheless, the bacterial communities were quite similar in GAC attached and suspended samples regarding bacterial phylum structure.

Fig. 4.7.(b) shows the relative abundance of bacterial community at the genus level. Notably, with GAC addition, *Syntrophomonas* genus substantially increased in relative abundance compared to control and magnetite amended reactors (11% vs. 4-7%), which was known as syntrophic LCFA β -oxidizing bacteria (Ziels et al., 2016). The enrichment of *Syntrophomonas* within the bacteria community was also corroborated by 16S rRNA gene qPCR results (3.8×10^8 cells g^{-1} GAC vs. 1.3 - 1.7×10^7 cells mL^{-1}). With GAC addition, more abundant and diverse fermentative bacteria were also enriched, including *Aminobacterium*, *Tepidimicrobium*, T78, *Pelomaculum*, *Ruminococcus*, *Clostridium*, and *Caldicoprobacter*, as well as many undefined genera belonging to order SHA-98 and family *Porphyromonadaceae*. For instance, the genus *Aminobacterium* (phylum *Synergistetes*) can ferment amino acids to acetate, propionate and hydrogen (Y.-F. Li et al., 2015). In contrast, *Thermacetogenium* and candidate genus S1, both of which contain syntrophic acetate-

oxidizing bacteria (Hattori et al., 2000; Sasaki et al., 2011), were in higher abundance in both control and magnetite reactors. The results indicated that non-acetoclastic oxidative pathway might dominate in control and magnetite reactors utilizing acetate, which was recognized as rate-limiting and might explain their acetate accumulations (Y.-F. Li et al., 2015; Lin et al., 2017).

Fig. 4.7.(c) shows the relative abundance of methanogens at the genus level. *Methanosarcina* and *Methanoculleus* were the two most dominant genera (together >86%) in all bioreactors. The relative abundance of *Methanosarcina* was the highest in control (93%), followed by magnetite (81%), and GAC (42–55%) reactors. While the proportion of *Methanoculleus*, known as hydrogenotrophic methanogens, was the highest in GAC (42–44%), followed by magnetite (18%) and control (7%) reactors. Other H₂-utilizing methanogens such as *Methanobacterium* was also present at low relative abundance in magnetite and GAC amended reactors. Considering the abundance of methanogens, *Methanosarcina* (GAC: 7.0×10^8 cells g⁻¹ GAC, magnetite: 3.4×10^7 cells mL⁻¹, control: 2.8×10^7 cells mL⁻¹), *Methanoculleus* (GAC: 5.5×10^8 cells g⁻¹ GAC, magnetite: 7.6×10^6 cells mL⁻¹, control: 2.1×10^6 cells mL⁻¹), and *Methanobacterium* (GAC: 1.1×10^7 cells g⁻¹ GAC, magnetite: 3.9×10^5 cells mL⁻¹, control: 0) were greatly enriched with the addition of GAC and magnetite over control. *Methanoculleus* increased to a higher degree than other two genera, resulting in a higher relative abundance in GAC and magnetite amended reactors compared to control. Acetoclastic methanogens are believed to be the most sensitive group to LCFA toxicity (Ziels et al., 2016), probably explained the absence of *Methanosaeta* in this study. Several recent studies have previously reported the abundance of *Methanosarcina* in co-digestion of FOG (Yamrot M. Amha et al., 2017), while *Methanosarcina* spp. are metabolically versatile and can shift the methanogenic pathway from acetoclastic to hydrogenotrophic methanogenesis as the level of acid or ammonia increased (Kurade et al., 2019).

Overall, substantial changes in the bacterial and archaeal community abundance and structure were observed with GAC and magnetite addition. GAC addition enriched more abundant and diverse bacteria and methanogens than control. Magnetite addition also showed similar trends but to a lesser degree. The formation of methane from LCFA involves a syntrophic partnership of proton-reducing acetogenic bacteria, which utilize the β -oxidation pathway to convert LCFA into acetate and formate/hydrogen, along with hydrogenotrophic and/or acetoclastic methanogens (Ziels et al., 2016). Thus, the substantial enrichment of syntrophic LCFA β -oxidizing bacteria (e.g. *Syntrophomonas*) and methanogenic archaea (e.g. *Methanosarcina* and *Methanoculleus*) in the GAC amended reactor likely attributed to the superior methanogenesis kinetics. Furthermore, no appreciable increase in acetate was observed with GAC addition although β -oxidation bacteria increased, suggesting that acetate was efficiently degraded in GAC-amended reactor. Previous studies have also suggested that enhanced biomethane production could be achieved by promoting a higher biomass of slow-growing syntrophic consortia (Ziels et al., 2016).



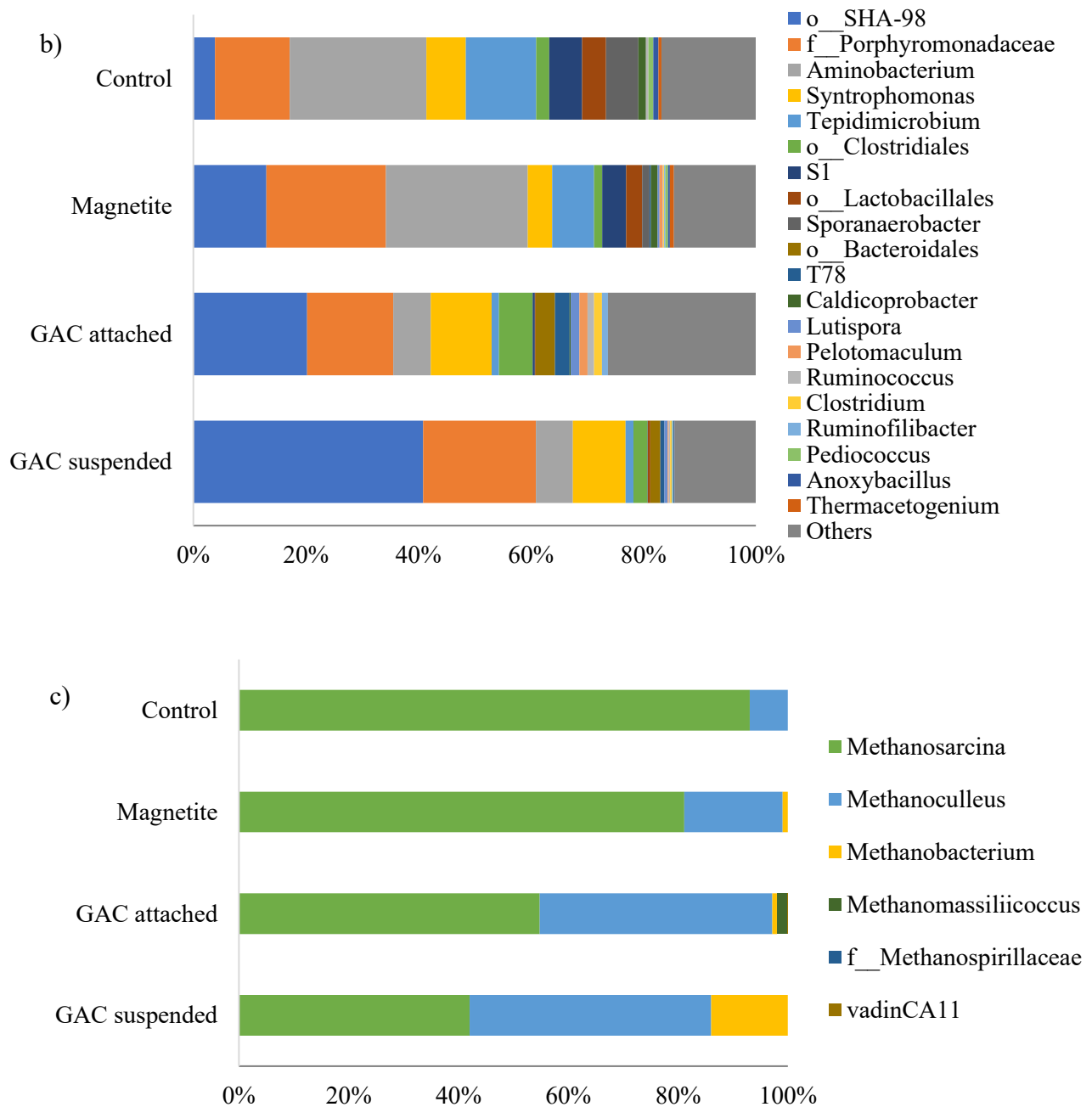


Fig 4.7. Relative abundance of (a) bacterial community at phylum level, (b) bacterial community at genus level and (c) methanogens at genus level. Note: sequences that accounted for less than 1% of their population were grouped into “Others”.

In addition to retention of active biomass, microbes attached to GAC may also reduce the interspecies distance, thereby enhancing the mass transfer (i.e. acids, H₂) and stimulating more diverse bacteria (Barua and Dhar, 2017). Moreover, previous studies suggested that the addition of conductive materials could facilitate enrichment of electroactive syntrophic bacteria (e.g., *Geobacter*) capable of transferring electrons to methanogens, which is known as direct interspecies electron transfer (DIET) (Crest et al., 2018; Dang et al., 2016; Lin et al., 2018a; Zhao et al., 2017b). As no apparent electro-active bacteria were detected in this study, we can conclude that conductive materials served more as media for microbial aggregates instead of conductive conduit for promoting DIET. The complex of FW and FOG might limit the function of GAC as conductive conduit. For instance, lipid could adsorb around GAC surface, limiting the direct contact of electroactive microbes with GAC (J. Hunter Long et al., 2012).

Chapter 5

Conclusions and Outlook

5.1 Conclusions

The optimal mixing ratio of 70%FW and 30%FOG was obtained, which was 1.2 times and 12 times of that obtained from digestion of FW and FOG alone, respectively. The fed-batch results showed GAC substantially reduced the lag phase, alleviated VFA accumulation, and improved the methane production rate compared to control and magnetite bioreactor. The FTIR spectra also suggested a decreasing trend in degradation of lipids, protein and carbohydrates in GAC, magnetite and control reactors. The microbial results showed that GAC addition enriched more abundant and diverse bacteria (e.g. LCFA β -oxidizing bacteria *Syntrophomonas*) and methanogens (e.g. *Methanosarcina* and *Methanoculleus*) than control and magnetite reactor, likely attributed to the superior methanogenesis kinetics in GAC amended bioreactor. Our findings suggest that the addition of GAC could provide a sustainable strategy to enrich kinetically efficient syntrophic microbiome to favor methanogenesis kinetics in co-digestion of FW and FOG.

5.2 Significance of results and outlook

Full-scale co-digestion of FOG with sewage sludge has been successfully implemented in many wastewater treatment plants across the world. But there is very limited information regarding the co-digestion of FOG with FW in full-scale application. The practical co-digestion cases of FOG with sludge showed 32-82% increases in gas production[57]. However, most of the full-scale processes required 25–50 days for FOG biodegradation depending upon the concentration of FOG [58]. Several pretreatment methods, such as mechanical, chemical, and biological processes or combination of these, have been reported to shorten lag phase and retention time for FOG digestion

[59,60], which require either high energy input or chemicals consumption. While in this study, lag phase has been significantly reduced with addition of conductive additives, which can be recycled and thereby only requiring initial investment. However, this study was conducted in fed-batch mode, while retention and recycle of GAC and magnetite in continuous anaerobic digester must be implemented to make this approach economically feasible, which warrants further studies.

5.3 Recommendations

- Long term continuous operation needed to be conducted with high loading of FOG and food waste to further evaluate the process performance.
- Low cost conductive additive such as biochar could be investigated to observe the effects on overall efficiency of co-digestion of FOG and food waste.

References

1. Alqaralleh, R.M., Kennedy, K., Delatolla, R., Sartaj, M., 2016. Thermophilic and hyper-thermophilic co-digestion of waste activated sludge and fat, oil and grease: Evaluating and modeling methane production. *J. Environ. Manage.* 183, 551–561.
<https://doi.org/10.1016/j.jenvman.2016.09.003>
2. Alves, M Madalena, Pereira, M.A., Sousa, D.Z., Cavaleiro, A.J., Picavet, M., Smidt, H., Stams, A.J.M., 2009. Waste lipids to energy: How to optimize methane production from long-chain fatty acids (LCFA). *Microb. Biotechnol.* 2, 538–550.
<https://doi.org/10.1111/j.1751-7915.2009.00100.x>
3. Alves, M. Madalena, Pereira, M.A., Sousa, D.Z., Cavaleiro, A.J., Picavet, M., Smidt, H., Stams, A.J.M., 2009. Waste lipids to energy: How to optimize methane production from long-chain fatty acids (LCFA). *Microb. Biotechnol.* 2, 538–550.
<https://doi.org/10.1111/j.1751-7915.2009.00100.x>
4. Amha, Yamrot M., Sinha, P., Lagman, J., Gregori, M., Smith, A.L., 2017. Elucidating microbial community adaptation to anaerobic co-digestion of fats, oils, and grease and food waste. *Water Res.* 123, 277–289. <https://doi.org/10.1016/j.watres.2017.06.065>
5. Amha, Yamrot M, Sinha, P., Lagman, J., Gregori, M., Smith, A.L., 2017. Elucidating microbial community adaptation to anaerobic co-digestion of fats, oils, and grease and food waste. *Water Res.* 123, 277–289. <https://doi.org/10.1016/j.watres.2017.06.065>
6. Angelidaki, I., Sanders, W., 2004. Assessment of the anaerobic biodegradability of macropollutants. *Rev. Environ. Sci. Bio/Technology* 3, 117–129.
<https://doi.org/10.1007/s11157-004-2502-3>
7. Barua, S., Dhar, B.R., 2017. Advances towards understanding and engineering direct

- interspecies electron transfer in anaerobic digestion. *Bioresour. Technol.* 244, 698–707.
<https://doi.org/10.1016/j.biortech.2017.08.023>
8. Bridges, O., 2003. Double trouble: Health risks of accidental sewage release. *Chemosphere*. [https://doi.org/10.1016/S0045-6535\(03\)00472-7](https://doi.org/10.1016/S0045-6535(03)00472-7)
 9. Callahan, B.J., McMurdie, P.J., Rosen, M.J., Han, A.W., Johnson, A.J.A., Holmes, S.P., 2016. DADA2: high-resolution sample inference from Illumina amplicon data. *Nat. Methods* 13, 581. <https://doi.org/10.1038/nmeth.3869>
 10. Caporaso, J.G., Kuczynski, J., Stombaugh, J., Bittinger, K., Bushman, F.D., Costello, E.K., Fierer, N., Peña, A.G., Goodrich, J.K., Gordon, J.I., Huttley, G.A., Kelley, S.T., Knights, D., Koenig, J.E., Ley, R.E., Lozupone, C.A., McDonald, D., Muegge, B.D., Pirrung, M., Reeder, J., Sevinsky, J.R., Turnbaugh, P.J., Walters, W.A., Widmann, J., Yatsunenko, T., Zaneveld, J., Knight, R., 2010. QIIME allows analysis of high-throughput community sequencing data. *Nat. Methods* 7, 335–336.
<https://doi.org/10.1038/nmeth.f.303>
 11. Capson-Tojo, G., Rouez, M., Crest, M., Steyer, J.-P., Delgenès, J.-P., Escudié, R., 2016. Food waste valorization via anaerobic processes: a review. *Rev. Environ. Sci. Bio/Technology* 15, 499–547. <https://doi.org/10.1007/s11157-016-9405-y>
 12. Carrere, H., Rafrafi, Y., Battimelli, A., Torrijos, M., Delgenes, J.P., Motte, C., 2012. Improving methane production during the codigestion of waste-activated sludge and fatty wastewater: Impact of thermo-alkaline pretreatment on batch and semi-continuous processes. *Chem. Eng. J.* 210, 404–409. <https://doi.org/10.1016/J.CEJ.2012.09.005>
 13. Castaldi, P., Alberti, G., Merella, R., Melis, P., 2005. Study of the organic matter evolution during municipal solid waste composting aimed at identifying suitable

- parameters for the evaluation of compost maturity. *Waste Manag.* 25, 209–213.
<https://doi.org/10.1016/j.wasman.2004.12.011>
14. Chowdhury, B., Lin, L., Dhar, B.R., Islam, M.N., McCartney, D., Kumar, A., 2019. Enhanced biomethane recovery from fat, oil, and grease through co-digestion with food waste and addition of conductive materials. *Chemosphere* 236, 124362.
<https://doi.org/10.1016/J.CHEMOSPHERE.2019.124362>
15. Crest, M., Bernet, N., Trably, E., Santa-Catalina, G., Moscoviz, R., Escudié, R., Steyer, J.-P., Delgenès, J.-P., Ruiz, D., Capson-Tojo, G., Rouez, M., 2018. Addition of granular activated carbon and trace elements to favor volatile fatty acid consumption during anaerobic digestion of food waste. *Bioresour. Technol.* 260, 157–168.
<https://doi.org/10.1016/j.biortech.2018.03.097>
16. Cruz Viggì, C., Rossetti, S., Fazi, S., Paiano, P., Majone, M., Aulenta, F., 2014. Magnetite particles triggering a faster and more robust syntrophic pathway of methanogenic propionate degradation. *Environ. Sci. Technol.* 48, 7536–7543.
<https://doi.org/10.1021/es5016789>
17. Cuetos, M.J., Morán, A., Otero, M., Gómez, X., 2009. Anaerobic co-digestion of poultry blood with OFMSW: FTIR and TG-DTG study of process stabilization. *Environ. Technol.* 30, 571–582. <https://doi.org/10.1080/09593330902835730>
18. Da Silva Almeida, H., Corrêa, O.A., Eid, J.G., Ribeiro, H.J., De Castro, D.A.R., Pereira, M.S., Pereira, L.M., De Andrade Mâncio, A., Santos, M.C., Da Silva Souza, J.A., Borges, L.E.P., Mendonça, N.M., Machado, N.T., 2016. Production of biofuels by thermal catalytic cracking of scum from grease traps in pilot scale. *J. Anal. Appl. Pyrolysis* 118, 20–33. <https://doi.org/10.1016/j.jaap.2015.12.019>

19. Dang, Y., Holmes, D.E., Zhao, Z., Woodard, T.L., Zhang, Y., Sun, D., Wang, L.-Y., Nevin, K.P., Lovley, D.R., 2016. Enhancing anaerobic digestion of complex organic waste with carbon-based conductive materials. *Bioresour. Technol.* 220, 516–522. <https://doi.org/10.1016/J.BIORTECH.2016.08.114>
20. Dang, Y., Sun, D., Woodard, T.L., Wang, L.-Y., Nevin, K.P., Holmes, D.E., 2017. Stimulation of the anaerobic digestion of the dry organic fraction of municipal solid waste (OFMSW) with carbon-based conductive materials. *Bioresour. Technol.* 238, 30–38. <https://doi.org/10.1016/j.biortech.2017.04.021>
21. Das, A., Mondal, C., 2015. Comparative Kinetic Study of Anaerobic Treatment of Thermally Pretreated Source-Sorted Organic Market Refuse. *J. Eng. (United States)* 2015. <https://doi.org/10.1155/2015/684749>
22. Davidsson, Å., Lövestedt, C., la Cour Jansen, J., Gruvberger, C., Aspegren, H., 2008. Co-digestion of grease trap sludge and sewage sludge. *Waste Manag.* 28, 986–992. <https://doi.org/10.1016/J.WASMAN.2007.03.024>
23. Del Mundo, D.M.N., Sutheerawattananonda, M., 2017. Influence of fat and oil type on the yield, physico-chemical properties, and microstructure of fat, oil, and grease (FOG) deposits. *Water Res.* 124, 308–319. <https://doi.org/10.1016/j.watres.2017.07.047>
24. Dhar, B.R., Elbeshbishy, E., Hafez, H., Nakhla, G., Ray, M.B., 2011. Thermo-oxidative pretreatment of municipal waste activated sludge for volatile sulfur compounds removal and enhanced anaerobic digestion. *Chem. Eng. J.* 174. <https://doi.org/10.1016/j.cej.2011.08.070>
25. Dhar, B.R., Nakhla, G., Ray, M.B., 2012. Techno-economic evaluation of ultrasound and thermal pretreatments for enhanced anaerobic digestion of municipal waste activated

- sludge. *Waste Manag.* 32, 542–549. <https://doi.org/10.1016/j.wasman.2011.10.007>
26. Florentino, A.P., Sharaf, A., Zhang, L., Liu, Y., 2019. Overcoming ammonia inhibition in anaerobic blackwater treatment with granular activated carbon: the role of electroactive microorganisms. *Environ. Sci. Water Res. Technol.* 5, 383–396. <https://doi.org/10.1039/C8EW00599K>
27. Galbraith, H., Miller, T.B., 1973. Physicochemical Effects of Long Chain Fatty Acids on Bacterial Cells and their Protoplasts. *J. Appl. Bacteriol.* 36, 647–658. <https://doi.org/10.1111/j.1365-2672.1973.tb04150.x>
28. Girault, R., Bridoux, G., Nauleau, F., Poullain, C., Buffet, J., Peu, P., Sadowski, A.G., Béline, F., 2012. Anaerobic co-digestion of waste activated sludge and greasy sludge from flotation process: Batch versus CSTR experiments to investigate optimal design. *Bioresour. Technol.* 105, 1–8. <https://doi.org/10.1016/J.BIORTECH.2011.11.024>
29. Gross, M.A., Jensen, J.L., Gracz, H.S., Dancer, J., Keener, K.M., 2017. Evaluation of physical and chemical properties and their interactions in fat, oil, and grease (FOG) deposits. *Water Res.* 123, 173–182. <https://doi.org/10.1016/j.watres.2017.06.072>
30. Grosser, A., Neczaj, E., 2016. Enhancement of biogas production from sewage sludge by addition of grease trap sludge. *Energy Convers. Manag.* 125, 301–308. <https://doi.org/10.1016/j.enconman.2016.05.089>
31. Hafidi, M., Amir, S., Revel, J.-C., 2005. Structural characterization of olive mill wastewater after aerobic digestion using elemental analysis, FTIR and ¹³C NMR. *Process Biochem.* 40, 2615–2622. <https://doi.org/10.1016/J.PROCBIO.2004.06.062>
32. Hattori, S., Kamagata, Y., Hanada, S., Shoun, H., 2000. *Thermacetogenium phaeum* gen. nov., sp. nov., a strictly anaerobic, thermophilic, syntrophic acetate-oxidizing bacterium.

- Int. J. Syst. Evol. Microbiol. 50, 1601–1609. <https://doi.org/10.1099/00207713-50-4-1601>
33. He, X., de los Reyes, F.L., Ducoste, J.J., 2017. A critical review of fat, oil, and grease (FOG) in sewer collection systems: Challenges and control. *Crit. Rev. Environ. Sci. Technol.* 47, 1191–1217. <https://doi.org/10.1080/10643389.2017.1382282>
34. He, X., de los Reyes, F.L., Leming, M.L., Dean, L.O., Lappi, S.E., Ducoste, J.J., 2013. Mechanisms of Fat, Oil and Grease (FOG) deposit formation in sewer lines. *Water Res.* 47, 4451–4459. <https://doi.org/10.1016/j.watres.2013.05.002>
35. He, X., Iasmin, M., Dean, L.O., Lappi, S.E., Ducoste, J.J., de los Reyes, F.L., 2011a. Evidence for Fat, Oil, and Grease (FOG) Deposit Formation Mechanisms in Sewer Lines. *Environ. Sci. Technol.* 45, 4385–4391. <https://doi.org/10.1021/es2001997>
36. He, X., Iasmin, M., Dean, L.O., Lappi, S.E., Ducoste, J.J., De Los Reyes, F.L., 2011b. Evidence for fat, oil, and grease (FOG) deposit formation mechanisms in sewer lines. *Environ. Sci. Technol.* 45, 4385–4391. <https://doi.org/10.1021/es2001997>
37. Husain, I.A.F., Alkhatib, M.F., Jami, M.S., Mirghani, M.E.S., Zainudin, Z. Bin, Hoda, A., 2014. Problems, control, and treatment of fat, oil, and grease (FOG): A review. *J. Oleo Sci.* 63, 747–752. <https://doi.org/10.5650/jos.ess13182>
38. Iasmin, M., Dean, L.O., Ducoste, J.J., 2016. Quantifying fat, oil, and grease deposit formation kinetics. *Water Res.* 88, 786–795. <https://doi.org/10.1016/j.watres.2015.11.009>
39. Kabouris*, J.C., Tezel, U., Pavlostathis, S.G., Engelmann, M., Todd, A.C., Gillette, R.A., 2008a. The Anaerobic Biodegradability of Municipal Sludge and Fat, Oil, and Grease at Mesophilic Conditions. *Water Environ. Res.* 80, 212–221. <https://doi.org/10.1016/j.crhy.2016.11.004>

40. Kabouris*, J.C., Tezel, U., Pavlostathis, S.G., Engelmann, M., Todd, A.C., Gillette, R.A., 2008b. The Anaerobic Biodegradability of Municipal Sludge and Fat, Oil, and Grease at Mesophilic Conditions. *Water Environ. Res.* 80, 212–221.
<https://doi.org/10.2175/106143007X220699>
41. Kabouris, J.C., Tezel, U., Pavlostathis, S.G., Engelmann, M., Dulaney, J., Gillette, R.A., Todd, A.C., 2009. Methane recovery from the anaerobic codigestion of municipal sludge and FOG. *Bioresour. Technol.* 100, 3701–3705.
<https://doi.org/10.1016/j.biortech.2009.02.024>
42. Karakashev, D., Batstone, D.J., Angelidaki, I., 2005. Influence of environmental conditions on methanogenic compositions in anaerobic biogas reactors. *Appl. Environ. Microbiol.* 71, 331–8. <https://doi.org/10.1128/AEM.71.1.331-338.2005>
43. Kataki, S., Hazarika, S., Baruah, D.C., 2017. Investigation on by-products of bioenergy systems (anaerobic digestion and gasification) as potential crop nutrient using FTIR, XRD, SEM analysis and phyto-toxicity test. *J. Environ. Manage.* 196, 201–216.
<https://doi.org/10.1016/j.jenvman.2017.02.058>
44. Keener, Kevin M., Ducoste, J.J., Holt, L.M., 2008. Properties Influencing Fat, Oil, and Grease Deposit Formation. *Water Environ. Res.* 80, 2241–2246.
<https://doi.org/10.2175/193864708x267441>
45. Keener, Kevin M, Ducoste, J.J., Holt, L.M., 2008. Properties influencing fat, oil, and grease deposit formation. *Water Environ. Res.* 80, 2241–6.
46. Kim, S.H., Han, S.K., Shin, H.S., 2004. Kinetics of LCFA Inhibition on Acetoclastic Methanogenesis, Propionate Degradation and β -Oxidation, in: *Journal of Environmental Science and Health - Part A Toxic/Hazardous Substances and Environmental*

- Engineering. pp. 1025–1037. <https://doi.org/10.1081/ESE-120028411>
47. Koster, I.W., Cramer, A., 1987. Inhibition of methanogenesis from acetate in granular sludge by long-chain fatty acids. *Appl. Environ. Microbiol.* 53, 403–409.
48. Kurade, M.B., Saha, S., Salama, E.-S., Patil, S.M., Govindwar, S.P., Jeon, B.-H., 2019. Acetoclastic methanogenesis led by *Methanosarcina* in anaerobic co-digestion of fats, oil and grease for enhanced production of methane. *Bioresour. Technol.* 272, 351–359. <https://doi.org/10.1016/J.BIORTECH.2018.10.047>
49. Li, C., Champagne, P., Anderson, B.C., 2015. Enhanced biogas production from anaerobic co-digestion of municipal wastewater treatment sludge and fat, oil and grease (FOG) by a modified two-stage thermophilic digester system with selected thermo-chemical pre-treatment. *Renew. Energy* 83, 474–482. <https://doi.org/10.1016/j.renene.2015.04.055>
50. Li, C., Champagne, P., Anderson, B.C., 2013. Effects of ultrasonic and thermo-chemical pre-treatments on methane production from fat, oil and grease (FOG) and synthetic kitchen waste (KW) in anaerobic co-digestion. *Bioresour. Technol.* 130, 187–197. <https://doi.org/10.1016/J.BIORTECH.2012.11.053>
51. Li, C., Champagne, P., Anderson, B.C., 2011a. Evaluating and modeling biogas production from municipal fat, oil, and grease and synthetic kitchen waste in anaerobic co-digestions. *Bioresour. Technol.* 102, 9471–9480. <https://doi.org/10.1016/j.biortech.2011.07.103>
52. Li, C., Champagne, P., Anderson, B.C., 2011b. Evaluating and modeling biogas production from municipal fat, oil, and grease and synthetic kitchen waste in anaerobic co-digestions. *Bioresour. Technol.* 102, 9471–9480.

<https://doi.org/10.1016/j.biortech.2011.07.103>

53. Li, Y.-F., Nelson, M.C., Chen, P.-H., Graf, J., Li, Y., Yu, Z., 2015. Comparison of the microbial communities in solid-state anaerobic digestion (SS-AD) reactors operated at mesophilic and thermophilic temperatures. *Appl. Microbiol. Biotechnol.* 99, 969–980. <https://doi.org/10.1007/s00253-014-6036-5>
54. Lienen, T., Kleyböcker, A., Verstraete, W., Würdemann, H., 2014. Foam formation in a downstream digester of a cascade running full-scale biogas plant: Influence of fat, oil and grease addition and abundance of the filamentous bacterium *Microthrix parvicella*. *Bioresour. Technol.* 153, 1–7. <https://doi.org/10.1016/j.biortech.2013.11.017>
55. Lin, L., Yu, Z., Li, Y., 2017. Sequential batch thermophilic solid-state anaerobic digestion of lignocellulosic biomass via recirculating digestate as inoculum – Part II: Microbial diversity and succession. *Bioresour. Technol.* 241, 1027–1035. <https://doi.org/10.1016/j.biortech.2017.06.011>
56. Lin, R., Cheng, J., Ding, L., Murphy, J.D., 2018a. Improved efficiency of anaerobic digestion through direct interspecies electron transfer at mesophilic and thermophilic temperature ranges. *Chem. Eng. J.* 350, 681–691. <https://doi.org/10.1016/j.cej.2018.05.173>
57. Lin, R., Cheng, J., Ding, L., Murphy, J.D., 2018b. Improved efficiency of anaerobic digestion through direct interspecies electron transfer at mesophilic and thermophilic temperature ranges. *Chem. Eng. J.* 350, 681–691. <https://doi.org/10.1016/j.cej.2018.05.173>
58. Liu, F., Rotaru, A.-E., Shrestha, P.M., Malvankar, N.S., Nevin, K.P., Lovley, D.R., 2012. Promoting direct interspecies electron transfer with activated carbon. *Energy Environ.*

- Sci. 5, 8982. <https://doi.org/10.1039/c2ee22459c>
59. Long, J. Hunter, Aziz, T.N., Reyes, F.L.D.L., Ducoste, J.J., 2012. Anaerobic co-digestion of fat, oil, and grease (FOG): A review of gas production and process limitations. *Process Saf. Environ. Prot.* 90, 231–245. <https://doi.org/10.1016/j.psep.2011.10.001>
60. Long, J Hunter, Aziz, T.N., Reyes, F.L.D.L., Ducoste, J.J., 2012. Anaerobic co-digestion of fat, oil, and grease (FOG): A review of gas production and process limitations. *Process Saf. Environ. Prot.* 90, 231–245. <https://doi.org/10.1016/j.psep.2011.10.001>
61. Lovley, D.R., 2006. Bug juice: harvesting electricity with microorganisms. *Nat. Rev. Microbiol.* 4, 497–508. <https://doi.org/10.1038/nrmicro1442>
62. Luostarinen, S., Luste, S., Sillanpää, M., 2009. Increased biogas production at wastewater treatment plants through co-digestion of sewage sludge with grease trap sludge from a meat processing plant. *Bioresour. Technol.* 100, 79–85.
<https://doi.org/10.1016/j.biortech.2008.06.029>
63. Madsen, M., Holm-Nielsen, J.B., Esbensen, K.H., 2011. Monitoring of anaerobic digestion processes: A review perspective. *Renew. Sustain. Energy Rev.*
<https://doi.org/10.1016/j.rser.2011.04.026>
64. Marlow, D.R., Boulaire, F., Beale, D.J., Grundy, C., Moglia, M., 2011. Sewer Performance Reporting: Factors That Influence Blockages. *J. Infrastruct. Syst.* 17, 42–51.
[https://doi.org/10.1061/\(ASCE\)IS.1943-555X.0000041](https://doi.org/10.1061/(ASCE)IS.1943-555X.0000041)
65. Martín-González, L., Castro, R., Pereira, M.A., Alves, M.M., Font, X., Vicent, T., 2011. Thermophilic co-digestion of organic fraction of municipal solid wastes with FOG wastes from a sewage treatment plant: Reactor performance and microbial community monitoring. *Bioresour. Technol.* 102, 4734–4741.

<https://doi.org/10.1016/j.biortech.2011.01.060>

66. Martínez, E.J., Fierro, J., Sánchez, M.E., Gómez, X., 2012. Anaerobic co-digestion of FOG and sewage sludge: Study of the process by Fourier transform infrared spectroscopy. *Int. Biodeterior. Biodegrad.* 75, 1–6.
<https://doi.org/10.1016/j.ibiod.2012.07.015>
67. Mata-Alvarez, J., Dosta, J., Romero-Güiza, M.S., Fonoll, X., Peces, M., Astals, S., 2014. A critical review on anaerobic co-digestion achievements between 2010 and 2013. *Renew. Sustain. Energy Rev.* 36, 412–427. <https://doi.org/10.1016/j.rser.2014.04.039>
68. Mata-Alvarez, J., Dosta, J., Romero-Güiza, M.S., Fonoll, X., Peces, M., Astals, S., 2014. A critical review on anaerobic co-digestion achievements between 2010 and 2013. *Renew. Sustain. Energy Rev.* 36, 412–427. <https://doi.org/10.1016/j.rser.2014.04.039>
69. Mata-Alvarez, J., Macé, S., Llabrés, P., 2000. Anaerobic digestion of organic solid wastes. An overview of research achievements and perspectives. *Bioresour. Technol.* 74, 3–16. [https://doi.org/10.1016/S0960-8524\(00\)00023-7](https://doi.org/10.1016/S0960-8524(00)00023-7)
70. Meissl, K., Smidt, E., Schwanninger, M., 2007. Prediction of humic acid content and respiration activity of biogenic waste by means of Fourier transform infrared (FTIR) spectra and partial least squares regression (PLS-R) models. *Talanta* 72, 791–799.
<https://doi.org/10.1016/j.talanta.2006.12.005>
71. Noutsopoulos, C., Mamais, D., Antoniou, K., Avramides, C., Oikonomopoulos, P., Fountoulakis, I., 2013. Anaerobic co-digestion of grease sludge and sewage sludge: The effect of organic loading and grease sludge content. *Bioresour. Technol.* 131, 452–459.
<https://doi.org/10.1016/J.BIORTECH.2012.12.193>
72. Pagés-Díaz, J., Westman, J., Taherzadeh, M.J., Pereda-Reyes, I., Sárvári Horváth, I.,

2015. Semi-continuous co-digestion of solid cattle slaughterhouse wastes with other waste streams: Interactions within the mixtures and methanogenic community structure. *Chem. Eng. J.* 273, 28–36. <https://doi.org/10.1016/j.cej.2015.03.049>
73. Palatsi, J., Illa, J., Prenafeta-Boldú, F.X., Laureni, M., Fernandez, B., Angelidaki, I., Flotats, X., 2010. Long-chain fatty acids inhibition and adaptation process in anaerobic thermophilic digestion: Batch tests, microbial community structure and mathematical modelling. *Bioresour. Technol.* 101, 2243–2251. <https://doi.org/10.1016/j.biortech.2009.11.069>
74. Pastore, C., Barca, E., Del Moro, G., Lopez, A., Mininni, G., Mascolo, G., 2015. Recoverable and reusable aluminium solvated species used as a homogeneous catalyst for biodiesel production from brown grease. *Appl. Catal. A Gen.* 501, 48–55. <https://doi.org/10.1016/j.apcata.2015.04.031>
75. Rajagopal, R., Massé, D.I., Singh, G., 2013. A critical review on inhibition of anaerobic digestion process by excess ammonia. *Bioresour. Technol.* 143, 632–641. <https://doi.org/10.1016/j.biortech.2013.06.030>
76. Rasit, N., Idris, A., Harun, R., Wan Ab Karim Ghani, W.A., 2015. Effects of lipid inhibition on biogas production of anaerobic digestion from oily effluents and sludges: An overview. *Renew. Sustain. Energy Rev.* 45, 351–358. <https://doi.org/10.1016/j.rser.2015.01.066>
77. Razaviarani, V., Buchanan, I.D., 2015. Calibration of the Anaerobic Digestion Model No. 1 (ADM1) for steady-state anaerobic co-digestion of municipal wastewater sludge with restaurant grease trap waste. *Chem. Eng. J.* 266, 91–99. <https://doi.org/10.1016/j.cej.2014.12.080>

78. Rinzema, A., Boone, M., van Knippenberg, K., Lettinga, G., 1994. Bactericidal effect of long chain fatty acids in anaerobic digestion. *Water Environ. Res.* 66, 40–49.
<https://doi.org/10.2175/wer.66.1.7>
79. Roy, F., Samain, E., Dubourguier, H.C., Albagnac, G., 1986. *Synthrophomonas sapovorans* sp. nov., a new obligately proton reducing anaerobe oxidizing saturated and unsaturated long chain fatty acids. *Arch. Microbiol.* 145, 142–147.
<https://doi.org/10.1007/BF00446771>
80. Ryue, J., Lin, L., Liu, Y., Lu, W., McCartney, D., Dhar, B.R., 2019. Comparative effects of GAC addition on methane productivity and microbial community in mesophilic and thermophilic anaerobic digestion of food waste. *Biochem. Eng. J.* 146, 79–87.
<https://doi.org/10.1016/j.bej.2019.03.010>
81. Salama, E.S., Saha, S., Kurade, M.B., Dev, S., Chang, S.W., Jeon, B.H., 2019a. Recent trends in anaerobic co-digestion: Fat, oil, and grease (FOG) for enhanced biomethanation. *Prog. Energy Combust. Sci.* 70, 22–42. <https://doi.org/10.1016/j.pecs.2018.08.002>
82. Salama, E.S., Saha, S., Kurade, M.B., Dev, S., Chang, S.W., Jeon, B.H., 2019b. Recent trends in anaerobic co-digestion: Fat, oil, and grease (FOG) for enhanced biomethanation. *Prog. Energy Combust. Sci.* 70, 22–42. <https://doi.org/10.1016/j.pecs.2018.08.002>
83. Sasaki, D., Hori, T., Haruta, S., Ueno, Y., Ishii, M., Igarashi, Y., 2011. Methanogenic pathway and community structure in a thermophilic anaerobic digestion process of organic solid waste. *J. Biosci. Bioeng.* 111, 41–46.
<https://doi.org/10.1016/j.jbiosc.2010.08.011>
84. Seghezze, L., Zeeman, G., Van Lier, J.B., Hamelers, H.V.M., Lettinga, G., 1998. A review: The anaerobic treatment of sewage in UASB and EGSB reactors. *Bioresour.*

Technol. [https://doi.org/10.1016/S0960-8524\(98\)00046-7](https://doi.org/10.1016/S0960-8524(98)00046-7)

85. Siriwongrungson, V., Zeng, R.J., Angelidaki, I., 2007. Homoacetogenesis as the alternative pathway for H₂ sink during thermophilic anaerobic degradation of butyrate under suppressed methanogenesis. *Water Res.* 41, 4204–4210.
<https://doi.org/10.1016/j.watres.2007.05.037>
86. Sousa, D.Z., Smidt, H., Alves, M.M., Stams, A.J.M., 2009. Ecophysiology of syntrophic communities that degrade saturated and unsaturated long-chain fatty acids. *FEMS Microbiol. Ecol.* 68, 257–272. <https://doi.org/10.1111/j.1574-6941.2009.00680.x>
87. Spaccini, R., Piccolo, A., 2008. Spectroscopic Characterization of Compost at Different Maturity Stages. *CLEAN – Soil, Air, Water* 36, 152–157.
<https://doi.org/10.1002/clen.200720012>
88. Stams, A.J.M., Plugge, C.M., 2009. Electron transfer in syntrophic communities of anaerobic bacteria and archaea. *Nat. Rev. Microbiol.* 7, 568–577.
<https://doi.org/10.1038/nrmicro2166>
89. Tandukar, M., Pavlostathis, S.G., 2015. Co-digestion of municipal sludge and external organic wastes for enhanced biogas production under realistic plant constraints. *Water Res.* 87, 432–445. <https://doi.org/10.1016/J.WATRES.2015.04.031>
90. Tu, Q., McDonnell, B.E., 2016. Monte Carlo analysis of life cycle energy consumption and greenhouse gas (GHG) emission for biodiesel production from trap grease. *J. Clean. Prod.* 112, 2674–2683. <https://doi.org/10.1016/J.JCLEPRO.2015.10.028>
91. Viswanathan, C. V., Bai, B.M., Pillai, S.C., n.d. Fatty Matter in Aerobic and Anaerobic Sewage Sludges. *J. (Water Pollut. Control Fed.* <https://doi.org/10.2307/25034584>
92. Wallace, T., Gibbons, D., O’Dwyer, M., Curran, T.P., 2017. International evolution of

- fat, oil and grease (FOG) waste management – A review. *J. Environ. Manage.* 187, 424–435. <https://doi.org/10.1016/J.JENVMAN.2016.11.003>
93. Wan, C., Zhou, Q., Fu, G., Li, Y., 2011. Semi-continuous anaerobic co-digestion of thickened waste activated sludge and fat, oil and grease. *Waste Manag.* 31, 1752–1758. <https://doi.org/10.1016/J.WASMAN.2011.03.025>
94. Wang, L., Aziz, T.N., de los Reyes, F.L., 2013. Determining the limits of anaerobic co-digestion of thickened waste activated sludge with grease interceptor waste. *Water Res.* 47, 3835–3844. <https://doi.org/10.1016/J.WATRES.2013.04.003>
95. Wang, T., Zhang, D., Dai, L., Dong, B., Dai, X., 2018. Magnetite Triggering Enhanced Direct Interspecies Electron Transfer: A Scavenger for the Blockage of Electron Transfer in Anaerobic Digestion of High-Solids Sewage Sludge. *Environ. Sci. Technol.* 52, 7160–7169. <https://doi.org/10.1021/acs.est.8b00891>
96. Williams, J.B., Clarkson, C., Mant, C., Drinkwater, A., May, E., 2012. Fat, oil and grease deposits in sewers: Characterisation of deposits and formation mechanisms. *Water Res.* 46, 6319–6328. <https://doi.org/10.1016/j.watres.2012.09.002>
97. Wu, L.J., Kobayashi, T., Kuramochi, H., Li, Y.Y., Xu, K.Q., Lv, Y., 2018. High loading anaerobic co-digestion of food waste and grease trap waste: Determination of the limit and lipid/long chain fatty acid conversion. *Chem. Eng. J.* 338, 422–431. <https://doi.org/10.1016/j.cej.2018.01.041>
98. Xu, R., Yang, Z., Chen, T., Zhao, L., Huang, J., Xu, H., Song, P., Li, M., 2015a. Anaerobic co-digestion of municipal wastewater sludge with food waste with different fat, oil, and grease contents: Study of reactor performance and extracellular polymeric substances. *RSC Adv.* 5, 103547–103556. <https://doi.org/10.1039/c5ra21459a>

99. Xu, R., Yang, Z., Chen, T., Zhao, L., Huang, J., Xu, H., Song, P., Li, M., 2015b. Anaerobic co-digestion of municipal wastewater sludge with food waste with different fat, oil, and grease contents: study of reactor performance and extracellular polymeric substances. *RSC Adv.* 5, 103547–103556. <https://doi.org/10.1039/C5RA21459A>
100. Yang, Y., Zhang, Y., Li, Z., Zhao, Zhiqiang, Quan, X., Zhao, Zisheng, 2017a. Adding granular activated carbon into anaerobic sludge digestion to promote methane production and sludge decomposition. *J. Clean. Prod.* 149, 1101–1108. <https://doi.org/10.1016/j.jclepro.2017.02.156>
101. Yang, Y., Zhang, Y., Li, Z., Zhao, Zhiqiang, Quan, X., Zhao, Zisheng, 2017b. Adding granular activated carbon into anaerobic sludge digestion to promote methane production and sludge decomposition. *J. Clean. Prod.* 149, 1101–1108. <https://doi.org/10.1016/j.jclepro.2017.02.156>
102. Zhang, S., Chang, J., Lin, C., Pan, Y., Cui, K., Zhang, X., Liang, P., Huang, X., 2017. Enhancement of methanogenesis via direct interspecies electron transfer between Geobacteraceae and Methanosaetaceae conducted by granular activated carbon. *Bioresour. Technol.* 245, 132–137. <https://doi.org/10.1016/j.biortech.2017.08.111>
103. Zhang, W., Zhang, L., Li, A., 2015. Anaerobic co-digestion of food waste with MSW incineration plant fresh leachate: Process performance and synergistic effects. *Chem. Eng. J.* 259, 795–805. <https://doi.org/10.1016/j.cej.2014.08.039>
104. Zhao, Z., Li, Y., Quan, X., Zhang, Y., 2017a. Towards engineering application: Potential mechanism for enhancing anaerobic digestion of complex organic waste with different types of conductive materials. *Water Res.* 115, 266–277. <https://doi.org/10.1016/j.watres.2017.02.067>

105. Zhao, Z., Zhang, Y., Li, Y., Dang, Y., Zhu, T., Quan, X., 2017b. Potentially shifting from interspecies hydrogen transfer to direct interspecies electron transfer for syntrophic metabolism to resist acidic impact with conductive carbon cloth. *Chem. Eng. J.* 313, 10–18. <https://doi.org/10.1016/j.cej.2016.11.149>
106. Zhao, Z., Zhang, Y., Woodard, T.L., Nevin, K.P., Lovley, D.R., 2015. Enhancing syntrophic metabolism in up-flow anaerobic sludge blanket reactors with conductive carbon materials. *Bioresour. Technol.* 191, 140–145. <https://doi.org/10.1016/J.BIORTECH.2015.05.007>
107. Ziels, R.M., Karlsson, A., Beck, D.A.C., Ejlertsson, J., Yekta, S.S., Bjorn, A., Stensel, H.D., Svensson, B.H., 2016. Microbial community adaptation influences long-chain fatty acid conversion during anaerobic codigestion of fats, oils, and grease with municipal sludge. *Water Res.* 103, 372–382. <https://doi.org/10.1016/j.watres.2016.07.043>

Appendix A

Table A1. Results for modified Gompertz model fitting for each cycle.

Condition		Modified Gompertz model			
Cycle	Reactor	CH ₄ potential (L kg VS ⁻¹)	Maximum CH ₄ production rate (L kg VS ⁻¹ -d)	Lag phase (d)	R ²
1	Control	911.903	69.379	9.68	0.994
	Magnetite	791.016	80.659	8.46	0.996
	GAC	687.495	88.679	6.45	0.997
2	Control	1572.221	44.918	11.18	0.992
	Magnetite	904.597	59.674	8.79	0.994
	GAC	713.748	111.058	3.62	0.996
3	Control	862.431	48.772	6.41	0.997
	Magnetite	686.213	66.700	6.53	0.993
	GAC	694.259	116.453	2.03	0.995
4	Control	791.181	60.504	4.93	0.995
	Magnetite	740.525	72.706	6.81	0.994
	GAC	664.321	116.457	1.91	0.994
5	Control	660.703	76.428	4.58	0.993
	Magnetite	687.774	81.410	3.76	0.995
	GAC	659.178	106.649	1.23	0.998

Table A2. COD mass balance for different bioreactors from cycle-5.

Reactor	COD initial (mg)	COD Final (mg)	CH4 (ml)	CH4 (mg COD)	COD balance (%) ^a
GAC	40277±3015	20789±1392	8045	20370	102±1
Magnetite	44935±3860	22505±1244	8325	21076	97±1
Control	44915±1362	25538±2582	7788	19716	101±1

^aCOD balance (%) = [CH4 (mg COD) + COD final (mg)]/COD initial (mg)]

FOG deposit formation (Saponification reactions):



Methane bioconversion pathway

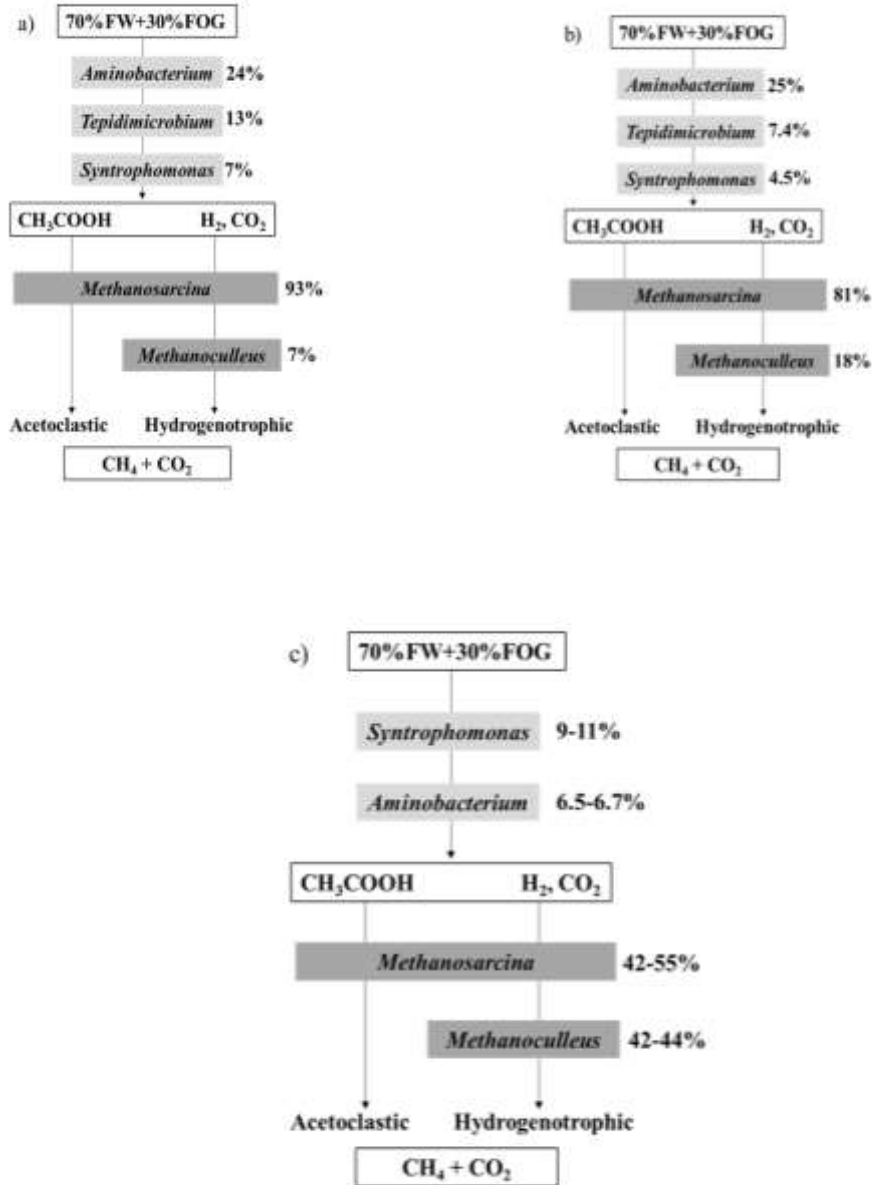


Fig. A1. Methane bioconversion pathway along with the key microorganisms in the co-digestion reactors: (a) control, (b) magnetite amended bioreactor, and (c) GAC amended bioreactor.